Memorial University of Newfoundland

Faculty of Engineering and Applied Science

Mechanical Design Project II – ENGI 8926

Design, Fabrication and Testing of a Water Current Energy Device

Team: M13

Team Members:

Richard Keough 200410769

Victoria Mullaley 200845279

Hilary Sinclair 200934859

Greg Walsh 200122786

Supervisor:

Dr. Michael Hinchey

April 4th, 2014

Abstract

River currents represent a reliable source of clean, renewable energy. While many devices have been designed to harness this energy, lift-based turbines represent the most efficient option for power generation. To optimize performance in low-speed currents, we propose the use of the Gorlov helical cross-flow turbine. The Gorlov helical design has been proven to perform in water currents, and has also been the basis of design for several wind turbines.

The Power Rangers design team has designed, built, and tested a scale model Gorlov helical cross-flow water turbine, and a similar turbine for use in air streams. SolidWorks CAD package was used to develop a virtual model for construction and virtual analysis. The resulting computer model was analyzed in Flow3D for hydrodynamic characteristics before construction of the physical model. Once acceptable virtual performance was obtained, the physical model was fabricated using rapid-prototype machines to print the ABS blades, and machined parts for blade and shaft mounting.

One prototype was tested in Memorial's wave/tow tank, while the other was tested in the university's wind tunnel. Trials were conducted for stream speeds of 0.25m/s to 2.0m/s in increments of 0.25m/s. For each speed trial, multiple tows were conducted with increasing brake torque, starting at zero (freewheel) and continuing until turbine was unable to rotate. Results of these tests were analyzed to produce Coefficient of Power vs. Coefficient of Speed, and Power vs. Angular Velocity curves for comparison with typical turbomachinery performance curves. The wind turbine was tested to determine self-starting capabilities and tip speed ratio (TSR).

The water turbine performed slightly better than expected in power generation, with lower efficiency than targeted. The maximum power output achieved was 13 Watts. Cp vs. Cs and Power vs. ω curves closely resembled those from more traditional turbine configurations. The wind turbine demonstrated self-starting capabilities, with a lower overall TSR than typical of water turbines, indicating the potential for an air-optimized helical turbine. From the test results, we believe the turbine constructed is a good starting point for future research in optimization.

Acknowledgements

We would like to extend our gratitude to our project supervisor, Dr. Michael Hinchey for the valuable advice and support that he has given us throughout each phase of the project. We would also like to thank Dr. S. Nakhla for providing us with knowledge relating to composite materials. Thanks also to Daniel Mackenzie and Michael Cousins for assisting us with Solidworks modeling and Finite Element Analysis of our turbine designs. We would also like to thank Brian Pretty, Steve Steele, Don Taylor, Bill Bidgood, Tom Pike and Caroline Koenig for assisting us in the fabrication of our turbine prototypes. Thanks also to Bradley Blake and Troy Freeborn from DJ Composites Inc. for designing the fabrication plan and fabricating three helical composite blades for our preliminary turbine design. We would also like to thank Trevor Clark and Craig Mitchell for assisting us with testing our turbine prototypes. Finally, thanks also to the NALCOR Community Outreach Program for helping fund the success of our project.

Table of Contents

List of Figures

List of Tables

List of Equations

1 Introduction

Four Senior Mechanical Engineering Students at Memorial University of Newfoundland formed the Power Rangers design team in August 2013. Together, the members of the Power Rangers bring a broad range of experience in areas such as project management, construction, testing and certification, and mechanical design. Our current project is to design, build and test a unique water current energy device. The team explored many design options to achieve the project objectives.

The team first developed a strategy to solve the design problem. The plan of action was to separate project tasks into the following three modules:

1. Research and Conceptual Design
2. Detailed Design
3. Fabrication and Testing

First, a conceptual design process was implemented. This allowed the team to extract a scoring formula from the analysis of project objectives and design constraints. Using this scoring formula, different design concepts were evaluated and the optimal water current energy device configuration was selected.

Next, the team designed the water current energy device. SolidWorks CAD package was used to develop a virtual model for construction and virtual analysis. The resulting computer model was analyzed in Flow3D for hydrodynamic characteristics and Finite Element Analysis (FEA) was performed before construction of the physical model. Once acceptable virtual performance was obtained, the physical prototypes were fabricated and subsequently tested.

Keeping on track with budget and schedule were integral to the success of our project. Economics and schedule adherence were evaluated at the research and concept selection phase, the detailed design phase as well as the fabrication and testing phase. By working efficiently as a cohesive team, we successfully designed, built and tested a unique water current energy device.

2 Problem Definition

The Power Rangers team has been tasked with designing, building and testing a unique water current energy device.

3 Design Objectives

The team determined the optimal water current energy device design configuration based on the project mission and constraints outlined below.

3.1 Mission

The water current energy device must:

1. be designed, fabricated and tested using available facilities as well as on site applications,

2. be novel in design or application,
3. successfully generate power from a flow of water,
4. be safe and environmentally friendly,
5. be implemented locally,
6. Self start.

3.2 Constraints

Design and fabrication options are limited by the following design constraints. The water current energy device must:

1. fit within the dimensions of testing facilities:
    a. Towing tank: 52m long x 5m wide x 3m deep with towing carriage capable of 5.0m/s maximum speed,
    b. Wind tunnel: 4' high x 3' wide,
2. fit within the dimensions of machining tools,
    a. Rapid prototyping machine: 16”x14”x16”,
3. be operable in a flow stream with a low cut-in speed,
4. be safe, both environmentally and structurally,
5. be constructed within a budget of $1000.

4 Background Research

Background research proved essential in the determination of the optimal water current energy device configuration. The team first researched how a water current energy device generates energy and the fluid mechanics behind the energy conversion.

4.1 Water to Wire Energy Conversion

Water current energy devices use kinetic energy created from the movement of water in river streams, tidal currents or other man made waterways to generate electricity (1). Systems take in power in the form of head and flow and deliver energy in the form of electricity. A water current energy device cannot harness the full energy potential of a current; these losses are due to friction, heating and noise in the system.

The mechanical framework of a water current energy device is composed of three main components; a turbine, a drive system and a generator. These components are shown below in Figure 1, as illustrated in the figure within the primary and secondary stages of electricity generation. As the current drives the turbine rotor, the kinetic energy of the current is converted into rotational energy of the turbine shaft. The drive system’s function is to transmit power from the turbine to the generator at the correct speed and direction for the generator. The drive system can use shafts, bearings, couplings, pulleys, gearboxes

and belts to achieve these objectives (2). The generator then converts its shaft rotational energy to electric energy. The tertiary step to deliver energy from "water to wire", as shown in Figure 1, includes the electrical system design. This stage is beyond the scope the Power Ranger's project goals.

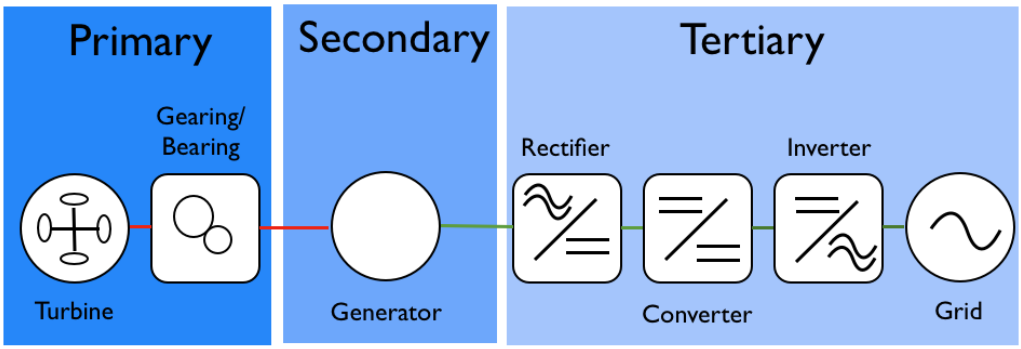

Figure 1: Water Current Energy Device System Overview (1)

Water current energy device design challenges to consider include foundation and mooring installation, maintenance requirements, cavitation, turbulence and biofouling. Special consideration should be made when designing the geometry of the turbine, choosing materials and selecting bearings (3). A water current energy device is a complex system and the design of such a system requires knowledge of fluid mechanics.

4.2 Fluid Mechanics

Fluid power mechanics involves the power that is available or can be added to a fluid. There are two types of turbomachines that accomplish this which are pumps and turbines. Pumps are designed to add power to a fluid, which will apply adequate pressure or head to a fluid. On the other hand, turbines extract energy from a moving fluid that can be converted to usable electrical energy (4). For example, pumps may be required in municipal water systems if there is not sufficient gravity, i.e. hydrostatic head, to distribute water adequately to consumers.

Turbomachines are also split into two categories, axial and radial. Axial turbomachines, such as a propeller turbine, have fluid moving in the direction of the shaft or drive axis. Radial turbomachines have fluid moving perpendicular to the shaft or drive system. Configurations where fluid motion that is both radial and axial contribute to the rotation of the turbine are considered to be cross flow turbines (4).

Traditional hydroelectric generation comes from high head application, where a height difference is achieved using a penstock connected to a lower elevation turbine which transfers the potential difference to consistent usable energy. The first application of hydroelectric generation in Newfoundland and Labrador occurred in Petty Harbour. This system was a traditional high-head application (5).

A new innovation is low-head power generation application. In this application, a water current energy device is designed to generate energy from the dynamic motion of the fluid. Low head, high velocity free-stream flow has energy that can rotate a turbine to generate power. The energy generated from such an application is governed by the following equation:

Equation 1: Turbine Power Equation

$$P = C_P \frac{1}{2} \rho A U^3$$

$$\begin{aligned}
&Where: \\
&P = power\,generation\ (Watts) \\
&C_P = Coefficient\,of\ turbine\,performance \\
&\rho = fluid\,density\ (kg/m^3) \\
&A = cross\,sectional\,area\,of\ turbine\,(m^3) \\
&U = fluid\,stream\,speed\ (m/s)
\end{aligned}$$

From Equation 1, it is clear that flow velocity, being the highest order term, is the driving force in power generation of the turbine.

5 Site Selection

The design problem states that the team must perform tests on a fabricated prototype. Therefore it is important to choose a potential energy site where we can perform on-site testing. The chosen site must be accessible, have a viable flow rate and optimal flow characteristics.

5.1 Site Generation

Research into the potential energy sources, based on flow velocity, is a necessity in selecting the site in which the turbine will be located. A viable current speed for the water current energy device to work and generate power is at least 2 m/s. Multiple energy sources were researched within Newfoundland and Labrador. These include ocean currents, tidal currents, and local rivers.

5.1.1 Newfoundland Ocean Currents

According to the Canada-Newfoundland and Labrador Offshore Petroleum Board (C-NLOPB), currents offshore Newfoundland are generally of very low speed. Measurements were taken in the Jeanne D'Arc Basin near the Hebron project at various depths which include near-surface (less than 30 meters deep), mid-depth (between 30 and 80 meters deep), and near bottom (greater than 80 meters deep) (6). The highest mean speed reached at these depth ranges was seen to be 19.0 cm/s while the highest maximum speed was 109.3 cm/s (7). Measurements were also taken in the Flemish Pass Basin near the Mizzen project at various depths ranging from 20m to 1150m. The highest mean speed reached at these depth ranges was seen to be 15.9 cm/s while the highest maximum speed was 50.4 cm/s (8). These currents have a much slower flow rate than the desired 2 m/s.

5.1.2 Newfoundland Tidal Currents

In 2006, National Research Council and the Canadian Hydraulics Centre identified 15 potential tidal current energy sites in Newfoundland. To identify these sites, they first identified passages and reaches with strong tidal currents and determined passage width, average depth and the maximum ebb and flood velocities during large tides. They then estimated the annual mean power density and annual mean power from the above mentioned parameters. It was determined that Newfoundland has a total

potential tidal current energy of 544 MW, with an average site size of 36 MW (9). Table 8, located in Appendix B, illustrates tidal current sites with current speed greater than 0.88 m/s. A disadvantage to designing a water current energy device specifically for implementation in a tidal current is that the design must account for bidirectional flow. To harness energy from both the ebb and flood flow, the turbine must be designed to operate bi-directionally.

5.1.3 Newfoundland Rivers

Historical flow data, summarizing average height and flow rate, are available online for a multitude of river systems. Data was analyzed and reviewed for multiple sites across the island (10). For testing purposes and ease of site selection, the team has decided to focus on inner-city rivers.

Rennie's River is a fairly small river, which runs from long pond southeast to Quidi Vidi Lake. It is of walking distance from Memorial University of Newfoundland and is approximately 2.5 km in length with varying widths and depths. Rennie's River is fed by the relatively large reservoir of Long Pond. It is expected that an inner-city river such as Rennie's River could produce a flow rate of 2-3 m/s in select locations.

5.2 Site Scoring Parameter Definition

To decide which site to move forward with, the three sites outlined previously were evaluated through a method called site scoring. Site scoring is a detailed screening system in which each site is analyzed individually based on the same criteria and then compared. Each site is given a score in relation to each criterion, and each criterion or parameter is given a level of significance or importance to the success of the project (11). The following are the site scoring parameters:

- **Accessibility:** Easy access to the site is required because the team plans to perform on-site testing once the prototype is fabricated. This parameter is given a weighting factor of 30% importance to the success of the project.

- **Flow Rate:** An optimal flow rate for the marine current energy device was selected to be greater than 2 m/s. This parameter is given a weighting factor of 60% importance to the success of the project.

- **Flow Characteristic:** Flow characteristic is an important factor because flow direction affects the complexity of the marine current energy device. Keeping the design simplistic is important, thus a unidirectional flow is more favourable than a bidirectional or omni-directional flow. This parameter is given a weighting factor of 10% importance to the success of the project.

These rankings are valued from 1 to 3, and the conditions that qualify each parameter for these rankings are outlined in Table 1 below.

Table 1: Site Selection Scoring Parameter Definition Table

Selection Criteria	Parameter 1	Parameter 2	Parameter 3
Accessibility	*Difficult to access potential energy site. Requires long commute by either vehicle, boat or plane.*	*Moderate accessibilty to potential energy site. Requires moderate commute.*	*Easy to access potential energy site. Requires short commute by vehicle or by foot.*
Flow Rate	*<1 m/s*	*1-2 m/s*	*>2 m/s*
Flow Characteristics	*Omnidirectional Flow*	*Bidirectional Flow (ebb and flood)*	*Unidirectional Flow*

5.3 Site Scoring Table

Once these conditions were defined for each contributing parameter, each design concept was analyzed individually based on these entries. A rank was assigned to the designs with respect to each parameter, and the weighting factor or level of importance was applied to each. From this process, a total ranking value was summed at the end of the analysis. These results were then compared side by side and the highest score was deemed the most feasible design to move forward with. This analysis can be seen in Table 2 below.

Table 2: Site Selection Concept Scoring

Selection Criteria	Weight	Tidal Current	Ocean Current	River
Accessibility	0.3	1	1	3
Flow Rate	0.6	3	1	3
Flow Characteristics	0.1	2	1	3
Total		2.3	1	3

Using the site scoring table, the river site achieved the highest total score. The team's turbine is designed for implementation in a river environment.

5.4 Selected Site Overview

An inner-city river such as Rennie's River has been selected as the optimal testing area for our turbine design. There are multiple advantages to the river site. Unlike tidal currents, there is no complexity of reversible current in a river. Additionally, within a river, there is more consistent flow rates and volumes than that of an unconstrained ocean current. A major advantage of choosing a river as the optimal site is the ease of onsite testing. We can freely test our prototype in a river stream with less constraints than if we were to test it in tidal or ocean currents.

Differing cross sections must be evaluated along the river profile so that enough room is available to submerge the turbine. Additionally, a relatively small river width of less than 5 meters should be sought out for ease in testing and installation of the prototype. The small river width also ensures a higher level of safety during the installation phase of the water current energy device.

6 Turbine Concept Selection

The following section provides an overview of the team's process and techniques of turbine concept selection.

6.1 Turbine Concept Generation

The team generated the following concepts after background research was completed. The team has decided to explore the configurations of five different water current turbines, as illustrated below in Figure 2.

(a) *(b)* *(c)* *(d)* *(e)*

Figure 2: Turbine Design Concepts (a) Auger Turbine (12), (b) Turbine Vent (13), (c) Savonius Turbine (14), (d) Darrieus Turbine (15), (e) Gorlov Turbine (16).

6.1.1 Auger Turbine

Traditionally used to lift water over 2500 years ago, the simplistic design of the auger turbine, as photographed in Figure 2a, rotates about its axis and physically moves water. The auger-type pump, often called Archimedes' screw has diverse applications due to its simplicity and reliability (17).

This type of primitive pump will turn in reverse when water flows over and through it, allowing for power generation. These types of turbines are becoming more common in green-energy applications. An example would be its use in the River Thames, supplying much of the power required by Buckingham Palace (18).

These turbine types are ideal in schemes which have low head and high flow, generating most of the power out of the velocity of the bulk flowing fluid, and not because of the potential energy difference (19).

The rotational speed of auger-type turbines is relatively low compared to other turbines. This quality combined with a large enough pitch and diameter will allow fish to swim through, unscathed, ultimately lowering the negative environmental impact.

Though the structure is not completely simple, as fabrication of a large screw could prove difficult, a modified purchased auger (e.g. Ice auger) could work for testing. These turbines are not unique for river design and have some of the oldest applications, this is a negative characteristic since a novel design is an objective of this project.

6.1.2 Turbine Vent

Turbine vents, as shown in Figure 2b, are mechanical devices for use in household or industrial application to aid mechanical systems. They are components of HVAC systems which use natural wind

energy to draw exhaust air through a system. One of the major drawbacks is their intermittency in that wind is never constant or predictable.

The turbine vent design is quite novel. Information regarding its application for micro-hydro power generation is not readily available. For power generation, it is considered a radial turbine as the rotation and fluid direction are perpendicular to the shaft. It is a modified Kaplan-type.

Designing such a device would not be difficult as they are relatively inexpensive and readily available for HVAC applications. This would remove a large portion of the mechanical design and fabrication aspect of the project, which would place more focus on idealization and testing. For use in rivers it would likely operate as a vertical axis turbine.

A negative aspect of this type of turbine is that it does not require a detailed mechanical design and fabrication plan due to the simplicity of design.

6.1.3 Savonius Turbine

The Savonius turbine, as shown in Figure 2c is a radial turbine designed for low speed flow. It is a drag-response turbine as drag forces on the blades, as opposed to lift forces, force the rotational motion of the turbine to generate power. The rotor is essentially two half-cylinders which are offset from each other to allow flow to be directed through the center and onto the opposite cylinder. This turbine's limited speed is due to drag forces resultant of the turbine's geometry. In addition, the Tip Speed Ratio (TSR) is limited to one.

Theory of Savonius rotors is taught at Memorial University of Newfoundland's fluids engineering department with focus on its low speed applications. The turbine itself benefits from a very low cut-in (start-up) speed and is well known to be self-starting. Its self-starting capabilities have been used in conjunction with non-self-starting turbines in order to avoid the requirement of input-power on start-up. An example would be a Darrieus rotor coupled with a Savonius rotor on the inside of the shaft. This accommodates the higher speed performance of the Darrieus rotor with the low-speed performance of the Savonius.

6.1.4 Darrieus Turbine

The Darrieus turbine, as shown in Figure 2d is traditionally used in wind applications though the same principles exist for hydro applications. The rotor is essentially shaped like an egg-beater and is a life device deriving its torque from the lift action of a moving fluid over an air or hydrofoil. In theory, the relatively high rotational speed of the Darrieus is advantageous because potentially more water energy can be extracted.

There are many variations of the Darrieus turbine and the amount of configurations are limitless. Common types of Darrieus rotors consist of two, three and four blades. These require careful balancing to avoid imbalance, vibrations and maintenance issues (20).

Darrieus turbines are commonly seen in vertical axis wind turbine (VAWT) applications. They are considered radial turbines as the fluid flow is normal to the direction of rotation. A more recent version of the Darrieus turbine modifies the blades orientation and is called the Gorlov helical turbine.

6.1.5 Gorlov Helical Turbine

Gorlov turbine, as shown in Figure 2e, is a Helical Darrieus-type turbine that incorporates both sweep and twist of the blades along an imaginary, cylindrical radius. The Gorlov is considered a cross-flow turbine due to the orientation of the blades (21).

Its helical design maintains that at some point along the blade's length, the ideal angle of attack is achieved for rotations. This achieves less pulsatory torque problems for a "smoother" drive. As well, for the same reasons, vibrations are mitigated which can lower maintenance and reliability problems. The helical design also achieves rotation regardless of flow direction (21).

With these properties in mind, the turbine can be used in any orientation in a flow that is normal to the shaft. This property increases its application potential – It can be mounted and working horizontally, vertically, or angled, assuming a low head application.

Little information is available regarding free-steam, micro-hydro applications for power generation but its potential exists. A river application is considered unique as the majority of applications are focused on very large-scale ocean currents or tidal movements.

6.2 Concept Scoring Parameter Definition

Similar to the previously discussed site scoring method, the team implemented turbine concept scoring to determine the optimal design for the project objectives. The five concepts outlined in the previous section were evaluated and analyzed individually based on the same criteria. The following are the turbine concept scoring parameters:

- **Constructability:** This refers to how easily the device can be designed and built. The simpler the process, the higher the score it receives. Similarly, if it is complex and complicated to fabricate it will receive a lower score. This parameter is given a weighting factor of 10% importance to the success of the project.

- **Reliability:** This refers to how often the device will need to be maintained and how well it could withstand harsh conditions. TSR is also a factor for determining reliability. TSR refers to the ratio of the turbine blade tip speed to the speed of the fluid flow (22). The higher the TSR and frequency of maintenance, as well as inability to withstand adverse conditions will result in a low score for reliability and vice versa to earn a high score. This parameter is given a weighting factor of 30% importance to the success of the project.

- **Efficiency:** This refers to the ratio of the turbine power to the power of the unconstrained uniform flow through the turbine area (23). The higher the efficiency, the higher the rating score. Greater than 25% was most desirable, while less than 20% was least desirable. This parameter is given a weighting factor of 30% importance to the success of the project.

- **Environmental Impact:** This refers to the negative effects the device could have on the environment and the potential environmental footprint that could be left due to its operations. The higher the impact to the environment such as marine life and extensive noise, the lower the rating score. The lower the impact, the higher the score (22). This parameter is given a weighting factor of 20% importance to the success of the project.

- **Design Experience Learning Potential:** This refers to the relative learning potential associated with the complexity and available information of the given design. With less information readily available, more contribution is given to the field of study and therefore increases the learning experience of the students. This results in a higher rating score. With more information readily available, less intuition is required from the students. This results in a lower rating score. This parameter is given a weighting factor of 10% importance to the success of the project.

The parameters are given a value ranking of 1,2, or 3. The conditions that qualify each parameter for these rankings are outlined in Table 3 below.

Table 3: Concept Scoring Parameters

	Parameter 1	Parameter 2	Parameter 3
Constructability	*Design requires complex materials and specialized machinery.*	*Relatively simple assembly using specialized machinery.*	*Easily and accurately constructed by hand with common materials; No specialized machinery needed.*
Reliability	*High TSR, requires servicing often, can not survive adverse conditions.*	*Moderate TSR, moderate servicing required.*	*Low TSR, requires minimal servicing, and a design that can survive adverse conditions such as loss of load.*
Efficiency	*Less than 20%*	*20-25%*	*Greater than 25%*
Environmental Impact	*Extensive harm to marine life, Extensive noise production, extensive impact to surrounding environment.*	*Moderate harm to marine life, moderate noise production, moderate impact to surrounding environment.*	*Minimal harm to marine life, minimal noise production, minimal impact surrounding environment.*
Design Experience	*Tried and proven design, tested in all marine environments.*	*Moderately researched design and tested in most marine environments.*	*Limited information available or studies completed on the design.*

6.3 Concept Scoring Table

The scoring table is illustrated below in Table 4. Each design was analysed based on the scoring parameters. Similar to the site scoring table, a rank was assigned to the designs with respect to each parameter, and the weighting factor or level of importance was applied to each. The scores of each turbine was summed and compared. The turbine with the highest score was chosen for the conceptual design.

Table 4: Concept Scoring Analysis Results

Selection Criteria	Weight	Darrius	Savonius	Gorlov Helical	Turbine Vent	Auger
Constructability	0.1	2	3	1	3	3
Reliability	0.3	1	3	2	1	2
Efficiency	0.3	2	1	3	1	2
Environmental Impact	0.2	2	2	2	1	3
Design Experience Learning Potential	0.1	1	1	3	3	1
Total		1.6	2	2.3	1.4	1.3

It can be seen that the Gorlov Helical Turbine design achieved the highest score through this analysis, and was therefore selected for design. This combination of Gorlov Helical Turbine design and a river setting has had limited application, thus making it a novel design.

6.4 Conceptual Design Summary

The Gorlov turbine, as shown in Figure 3, was developed by Alexander Gorlov, and patented over a series of patents from 1995 to 2001. This particular turbine is a lift-based reaction turbine, with roots in the Darrieus design, patented in 1931 (21). Like the Darrieus, the Gorlov utilizes foil-shaped blades to generate lift force from fluid flowing across the turbine. The resultant lift force applies a torque on the rotor, spinning it. As the turbine rotates, vector addition of fluid and rotor blade velocities determine lift and drag forces generated by the turbine blades. This caused some problems for the original twin-blade Darrieus design however, in that forces caused by free flow across the foils tended to oppose each other until enough rotational speed was built up for the rotor to generate lift due to momentum carrying them through these "dead spots", namely those where the foils generate no lift, but are subject to drag forces from the flowing stream fluid. On top of this, the two-bladed Darrieus tended to suffer from severe vibrations at speed due to torque fluctuations from the varying lift, depending on how the blades were positioned relative to the flow, generating maximum lift at the front and back of the rotation. These problems were remedied to an extent by creating multi-bladed Darrieus turbines, sometimes called gyromills. However, while increasing the number of blades lessened the problem, they were never solved in a satisfactory manner.

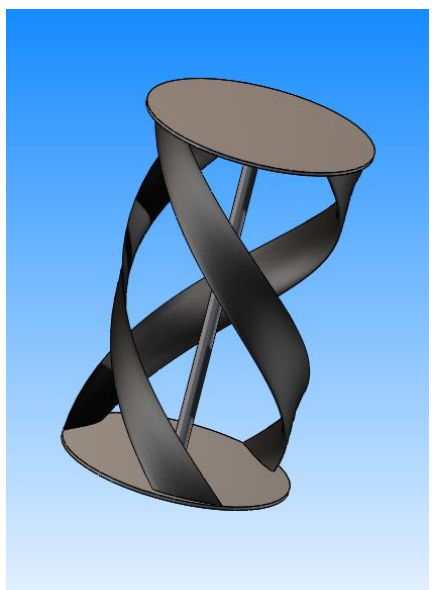

Figure 3: Gorlov Helical Turbine (30)

The Gorlov turbine took the practice of continually adding blades to a Darrieus one step farther. Instead of adding more and more blades with shorter and shorter arcs of separation, Gorlov essentially added an infinite number of infinitely thin blades through the use of a continuous profile helical blade. In this configuration, at any point in time some part of a blade is passing through any point in the plane of rotation, giving a smooth lift (and therefore torque) generation. This non-pulsating force means the Gorlov is not subject to vibration like the Darrieus, and is capable of self-starting, since lift generation is not dependant on the angular position of the blades. Furthermore, the helical blades can be engineered

to be part of the supporting structure, reducing the need for large hubs or guy wires, as required for other type installations. Finally, due to the arrangement of the blades, the Gorlov turbine rotates in the same direction, regardless of flow and can be mounted vertically, horizontally, or even on an incline, making it an ideal installation for a river current. See Figure 4 below for diagrams showing the apparent stream velocity, the sum of current and induced flow and resulting net force vectors. Note that this is for a tip speed ratio of unity, indicating larger net forces, and no "dead" zone for normal operating speeds.

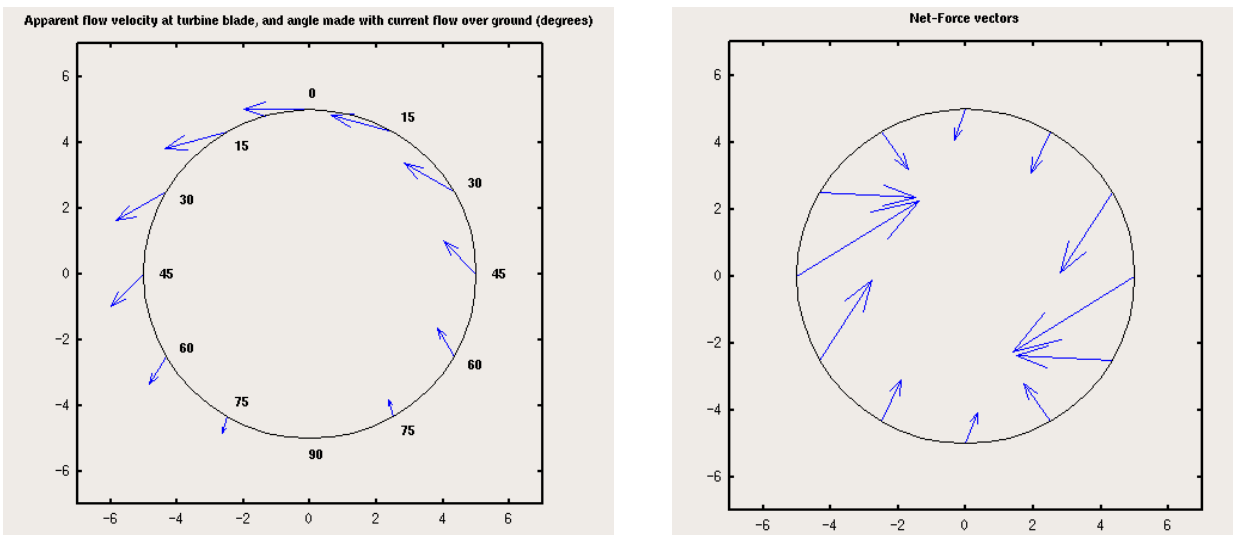

(a) *(b)*

Figure 4: Diagrams showing the apparent stream velocity, the sum of current and induced flow (a) and resulting net force vectors (b) (21).

7.0 Turbine Power Theory

According to Bernoulli, the energy of a fluid flow can be described by the equation:

Equation 2: Bernouilli's Equation

$$z + \frac{p}{\rho g} + \frac{V^2}{2g} = constant$$

Where: z is the fluid elevation relative to baseline, $\frac{p}{\rho g}$ is the water head pressure, and $\frac{V^2}{2g}$ is the kinetic head, or the amount of energy in moving fluid. Traditional turbines requiring hydro dams or other large civil works generally rely on slowing large amounts of fluid by restricting flow through a tube to generate a large pressure buildup behind a turbine which is then converted into rotational mechanical energy. In this case, the $\frac{V^2}{2g}$ term is negligible compared to the pressure head component. In stark contrast, turbines which harness low head free-steam energy such as the Darrieus or the Gorlov operate in situations where the $\frac{V^2}{2g}$ term (or the kinetic head), is dominant and the other two terms are

insignificant. These turbines allow large amounts of water to flow though, generating rotational force through harnessing the kinetic energy of the water (21).

To gain an understanding as to how much free-stream power can be captured by a turbine, one may start with the following equation, showing that the amount of energy contained in a fluid stream is:

$$Power = PQ$$

Where:

$P = Pressure$

$Q = Volumetric\ Flowrate$

Now with pressure as:

$$P = \rho \frac{U^2}{2}$$

And volumetric flow rate being:

$$Q = UA$$

Then the power available in a fluid stream is:

$$Power = \frac{1}{2}\rho A U^3$$

Where:

$\rho = fluid\ density$

$U = fluid\ stream\ velocity$

$A = cross\ sectional\ area\ of\ stream$

From this, it is possible to find the amount of energy a turbine is capable of extracting from the stream:

$$P = C_p \frac{1}{2}\rho A U^3$$

Where:

$P = power\ generation\ (Watts)$

$C_p = Coefficient\ of\ turbine\ performance$

$\rho = fluid\ density\ ({}^{kg}/_{m^3})$

$A = cross\ sectional\ area\ of\ turbine\ (m^3)$

$U = fluid\ stream\ speed\ ({}^{m}/_{s})$

With an experimentally proven efficiency of up to 35%, a predicted value of power generation for the Power Rangers prototype would be:

$$P = (.35)\left(\frac{1}{2}\right)\left(1000\,{}^{kg}/_{m^3}\right)(0.4064m)(0.2032m)(3\,{}^{m}/_{s})^3$$

$$P = 390\ watts$$

Using the same turbine size, a stream flowing at 5m/s would produce approximately 1800 watts of power.

8.0 Detailed Blade Design

The following section outlines the basis of our blade selection.

8.1 Preliminary Blade Design

While current literature describing the performance characteristics of lift-based helical turbines is limited, general trends in experimental and research results indicate that turbines with a high solidity ratio tend to have better start-up performance, and reach peak torque at a lower Tip Speed Ratio (TSR) than those turbines with lower solidity ratios. Some research indicates that solidity has a greater effect on turbine performance than that of the angle of attack of the blade foil. However, there is an upper limit on turbine solidity, as at some point fluid flow will tend to wholly "avoid" the object and flow around it, rather than interact with it. Accordingly, a preliminary design, as shown below in Figure 5, was chosen with σ = 0.30, a middle-of-the-pack solidity. This turbine should provide reasonable start-up torque, with good steady-state performance.

(a)

1:2 Aspect Ratio Turbine, Medium Solidity (Design I)	
Foil Shape	NACA 0018
Number of Blades	3
Solidity	0.3
Chord Length	0.0628 m
Aspect Ratio	1:02
Diameter	0.2 m
Height	0.4 m

(b)

Figure 5: Preliminary Turbine Design (Design I) (a) Solidworks model of NACA 0018 foil shape 0.3 solidity (b) Dimensions of blade with NACA 0018 foil shape 0.3 solidity

This design was sent to a local aerospace manufacturing company, DJ Composites Inc., for a recommendation on the feasibility of composite manufacturing, and for suggestions of design

considerations to take into account for composite construction. DJ Composites Inc. additionally agreed to fabricate the blades and provide information on the process to give insight into a comprehensive concept to the physical modelling procedure for composite manufacturing.

8.2 Detailed Blade Designs

As the design process continued, as shown below in Figure 6, it became apparent that a higher-solidity turbine would better match the required performance criteria.

Figure 6: Turbine Design Flow Chart

As a result, a decision was made to increase the turbine solidity to σ = 0.5. This constraint modification, along with our previously chosen constraints of height, diameter, and number of blades allowed the chord length of the foil to be calculated. The solidity, σ, of the turbine can be described as:

Equation 3: Turbine Solidity Equation

$$\sigma = \frac{CB}{2\pi R}$$

Where:

$$C = chord\ length\ of\ blade$$

$$B = number\ of\ blades$$

$$R = turbine\ radius$$

Manipulating, this gives:

$$C = \frac{2\sigma\pi R}{B}$$

For solidity of 0.5, radius of 0.100m, and 3 blades, this returns:

$$C = \frac{2(0.5)(\pi)(0.100m)}{3}$$

$$C = 0.1047m$$

Note that the solidity, σ, is independent of turbine height. In addition to the solidity, the helical angle, ϕ, was also required to produce a CAD model. If a turbine were to be "rolled out", the helical angle is the angle between the base, and the straight-line path of the blade.

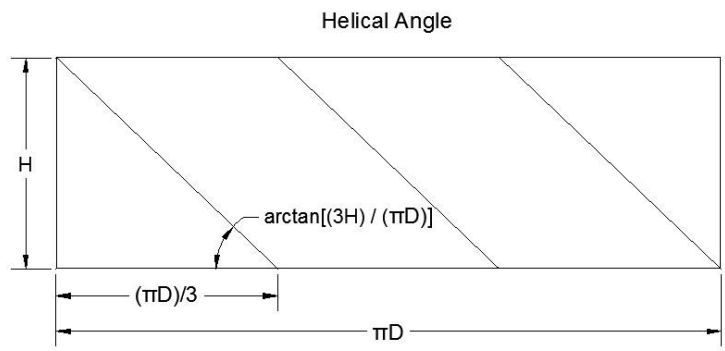

Figure 7: Helical Angle

This angle can be equated as:

Equation 4: Helical Angle Equation

$$\varphi = \arctan\left[\frac{Bh}{\pi D}\right]$$

Where:

$B = number\ of\ blades$

$h = turbine\ height$

$D = turbine\ diameter$

For the turbine of 0.400m height, 0.200m diameter, and with three blades, this gives:

$$\varphi = \arctan\left[\frac{(3)(0.400)}{(\pi)(0.200)}\right]$$

$$\varphi = 62.36°$$

However, after CFD analysis of this and several other turbines of the same aspect ratio, but with different solidities, it was recommended by the Project Supervisor to analyse a turbine with a 1:1 aspect ratio for comparison. This required a new helical angle, since it is dependent on the turbine height:

$$\varphi = \arctan\left[\frac{(3)(0.400)}{(\pi)(0.200)}\right]$$

$$\varphi = 43.67°$$

The resulting turbine of 0.200m height to 0.200m diameter, and solidity of 0.5 was, to date, the best performing turbine during start-up, and therefore was the turbine chosen for prototyping. The methodology behind the CFD analysis is explained in greater detail in section 8.3 Computational Fluid Dynamics, within this report. It was further recommended that we fabricate an additional turbine of identical foil and chord length with half the solidity, 0.25. This will allow us to compare the effects of different solidities on turbine performance. Both turbines, with blade designs II and III, are shown in Figure 8 and their dimensions are shown in Table 5.

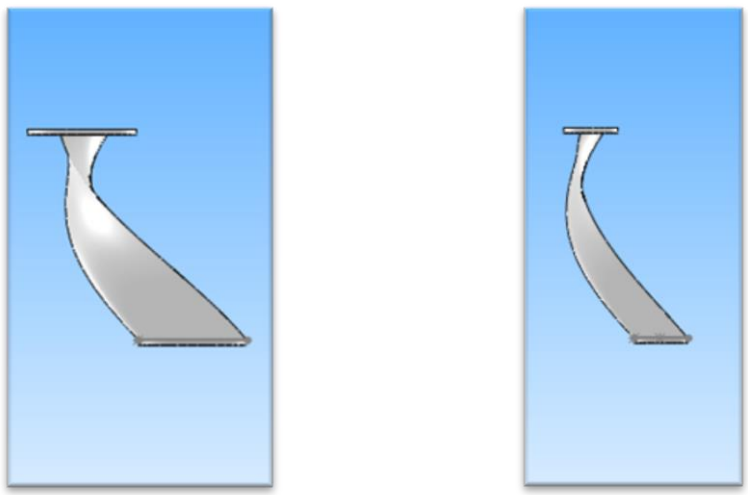

(a) *(b)*

Figure 8: Optimal Turbine Designs to Fabricate (a) NACA 0021, 0.5 Solidity (Design II) (b) NACA 0021, 0.25 Solidity (Design III)

Table 5: Blade Designs II & III Dimensions

	1:1 Aspect Ratio Turbine, High Solidity (Design II)	1:1 Aspect Ratio Turbine, Low Solidity (Design III)
Foil Shape	NACA 0021	NACA 0021
Number of Blades	3	3
Solidity	0.5	0.25
Chord Length	0.1047 m	0.0527 m
Aspect Ratio	1:01	1:01
Diameter	0.2 m	0.2 m
Height	0.2 m	0.2 m

8.3 Computational Fluid Dynamics

We completed CFD to choose the optimal turbine design based on torque and start-up capabilities. CFD is a subgenre of fluid mechanics which uses numerical models and numerical methods to determine fluid behaviour as a function of time. For each "cell" in a CFD analysis, various parameters such as velocities and pressure are calculated for that moment of time. These parameters are used to determine adjacent cells' parameters for the next time step and the model is iterated until a limit or prescribed finish time is achieved.

Due to the iterative nature of such calculations and the complicated equations that govern the flow characteristics, hand calculations are not feasible. This is because of the sheer number of calculations required and the inherent human error in hand calculations. Factors that affect our simulation are accuracy and time. As the size of a grid is decreased (greater number of iteration cells) the accuracy of the simulation is increased at the expense of longer simulation time.

CFD is an invaluable tool for engineers as it may take hours of hand-calculations for a very simple iteration, with the probability of a mistake increasing with complexity of model. CFD, in general, will decrease calculation time and increase accuracy.

8.3.1 Flow 3D

Flow 3D is a proprietary computer program that solves complex fluid calculations utilizing CFD principles. Flow 3D allows accurate modelling of real-life situations and presents the results in various ways including an attractive graphical user interface (GUI). The program can save a designer time and money because a physical model, testing apparatus, etc. are not required and, depending on the setup of the model, the results can be very similar to those physically tested.

Flow 3D has limitations for the student license with the maximum number of cells being 200,000. The faculty has access to a research license which we propose to use because the number of cells available (millions) will significantly increase the accuracy of results from the prototypes being fabricated. In this case, the vast increase in accuracy would be at the expense of simulation time (several days). The results presented in Flow 3D will be compared to the results achieved through physical testing.

The goals of running CFD in Flow 3D are to determine torque behaviour, angular velocity behaviour, and thus theoretical power output of the turbine. The specified parameters in Flow 3D are model type (6 tested), flow speed, fluid (water or air), and boundary conditions.

8.3.2 Starting Performance

Starting performance of any turbine or energy device is critical. To help maximize efficiency, external sources to help initiate rotation should be minimized. Part of our design objective is to design a turbine that will self-start. Though a difficult task, the twisted helical blades coupled with the 120 degree blade overlap lend themselves to better start-up torque than a traditional Darrieus rotor by always having at least one section of a blade in the optimum angle of attack relative to free-steam flow.

When there is zero torque applied to the turbine (ideal theoretical conditions), we achieve rotation. Running the simulation for several seconds until steady state is reached, we obtained a range of angular velocities. This is a range because of the periodic nature of turbine rotation. The value of steady state freewheel angular velocity was averaged to get a general idea of rotation. Half of the freewheel angular velocity yields maximum power output based on knowledge of turbine performance (4).

In all cases, simulating the largest and thickest of the foil shape (NACA 0021 with a solidity of 0.5) that we determined to be ideal (Design II), we achieved good start-up performance (turbine turned over). In contrast, when simulating the preliminary blade Design I, that is currently in the fabrication stage (NACA 0018 with a solidity of 0.3), we failed to achieve complete rotation. The turbine would only ineffectually rotate back and forth with an average of zero angular velocity in the Flow 3D model.

These simulation results were baffling as this turbine configuration was determined to be optimal during preliminary analysis. Upon critical evaluation of the Flow 3D model, we have concluded that the surrounding mesh was too coarse. We achieved rotation using the Design I configuration once we increased the number of simulation cells directly surrounding the turbine. The model which yielded zero rotation used the maximum number of cells available for that license (200,000). To increase the number of cells around the turbine, we had to use the research license for Flow 3D so that we could generate accurate results from our prototype using more representative conditions.

8.3.3 Torque Behavior

In turbine design as well as the accompanying shaft design, torque behaviour is of utmost importance. The shaft must be able to perform under the system's torque without failure while supplying smooth power transfer without too much bending. The torque applied to the shaft is due to the forces acting on the turbine blades and the resistance of the generator.

Generally, torque is equal to the force on the blades times the moment arm (radius from shaft to blade) and this value varies along the length of each blade. Power is then the overall turbine torque multiplied by the angular velocity of the turbine. Initially our determination of torque and rotational velocity behaviour were completed using Flow 3D.

The turbine model was imported into Flow 3D from SolidWorks by exporting a stereolithography (.stl) file format which basically approximates shapes as arrays of 2D planes (triangles). Flow 3D then allows the user to prescribe a fluid velocity (water at 2m/s) and simulates the fluid and structure interactions. By fixing rotation to only one axis, the model is run until steady state is reached and a freewheel velocity is obtained for each turbine configuration. Results of this analysis for the Design II turbine with a 1:1 aspect ratio and high solidity are shown below in Figure 9.

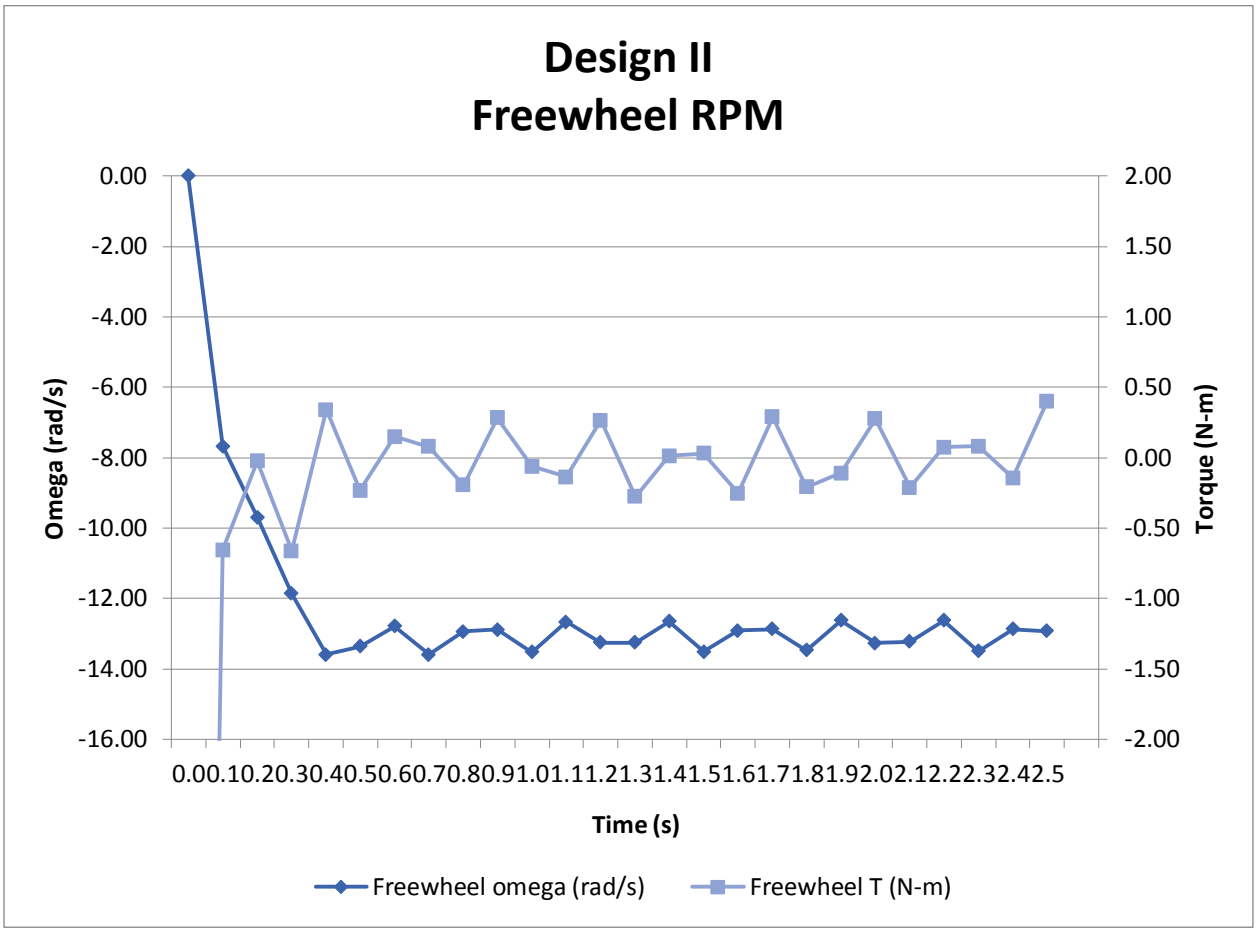

Figure 9: NACA 0021 0.5 Solidity Turbine Freewheel RPM (Design II)

The torque behaviour is simulated then by prescribing approximately half of the freewheel angular velocity and outputting the simulated torque associated with each turbine. Figure 10 shows the half-freewheel RPM for the Design II turbine blades with a 1:1 aspect ratio and high solidity.

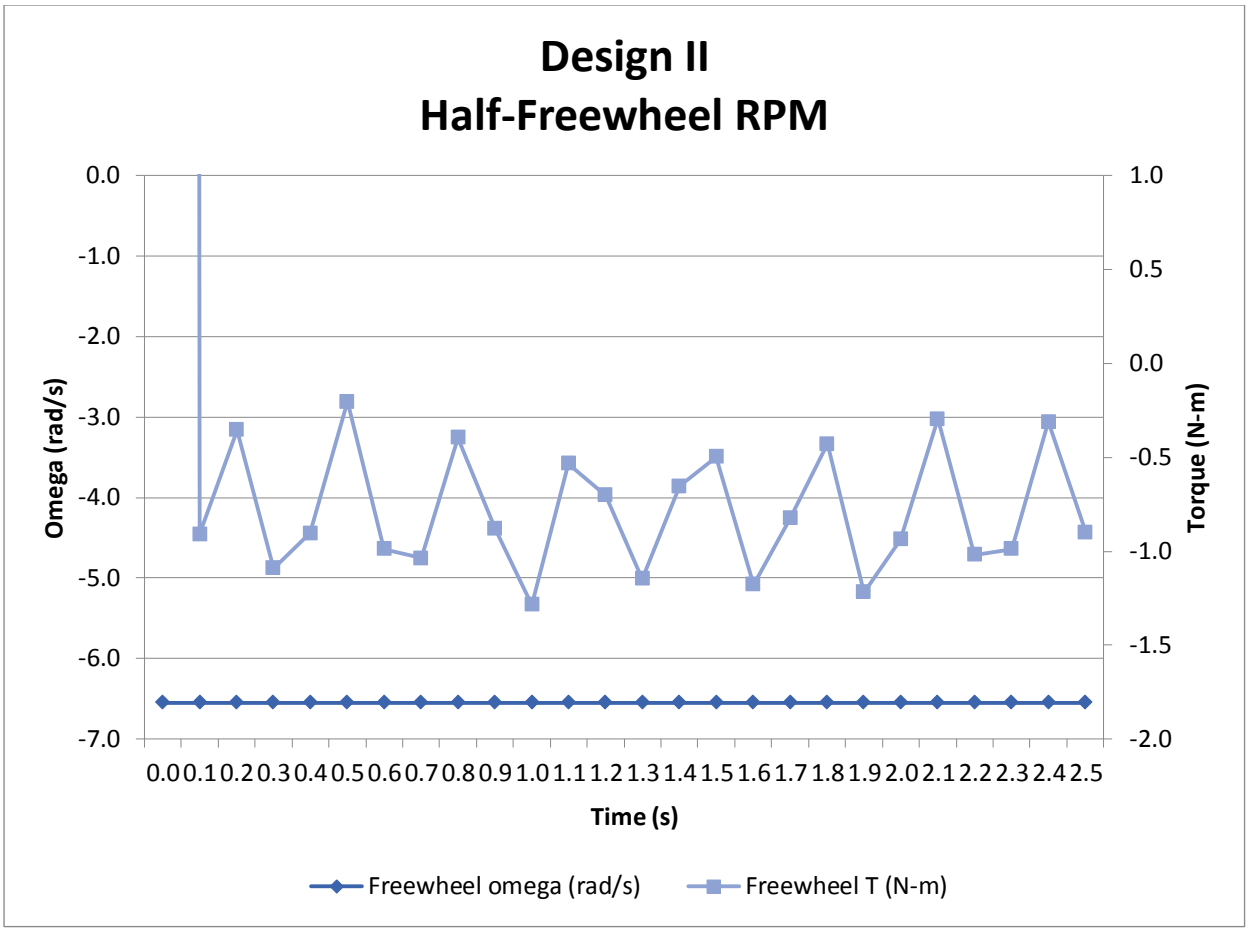

Figure 10: NACA 0021 0.5 Solidity Half-Freewheel RPM (Design II)

This optimum torque value is used to calculate the power coefficients for each configuration and generate power curves for each. The power curve displays both minimum values of power (at max torque, minimum angular velocity and vice versa) with the maximum power condition occurring somewhere close to the middle of these values. Figure 11 below shows the power curve for the Design II turbine with a 1:1 aspect ratio and high solidity.

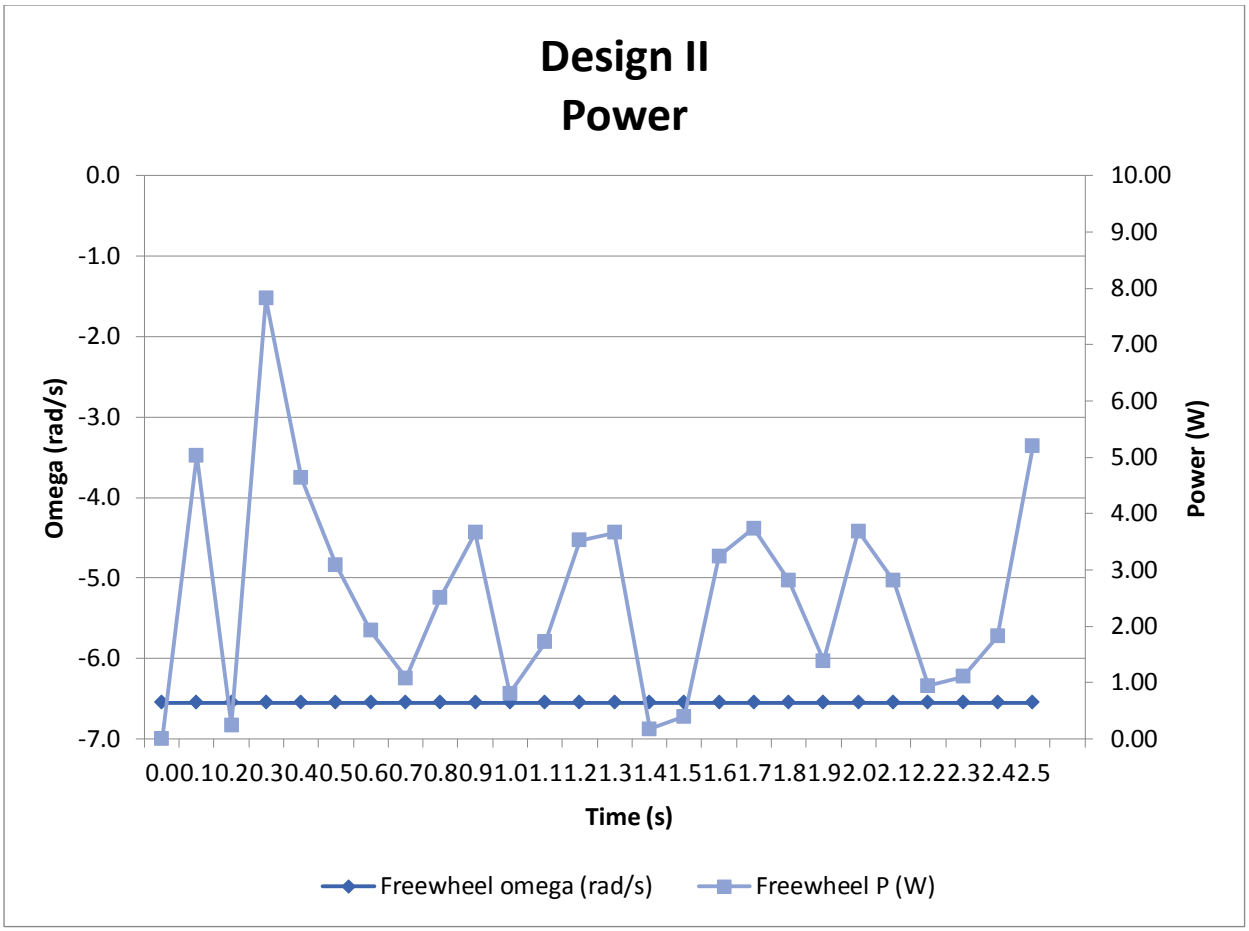

Figure 11: NACA 0021 0.5 Solidity Power curve (Design II)

Pressure distributions are required for use in FEA. Using Flow 3D and the NACA 0021 turbine with a solidity of 0.5 (Design II) we applied a water flow speed of 5 m/s, well above the design free-stream speed. From this analysis, we statically fixed the turbine blade and recorded the pressures along the blade length. This was done over 120 degrees of blade orientation and we recorded the largest pressure value the blade would experience. This gauge pressure is approximately 150,000 Pa.

Similarly for the 0.25 solidity NACA 0021 turbine (Design III), we applied a stream speed of 2m/s (as this blade is significantly smaller and, therefore, cannot withstand the same loads and noted the largest pressure. Using the same methodology described above, the only modifications being the stream speed and blade design, we noted a max gauge pressure of about 300 Pa.

8.4 Finite Element Analysis

FEA was performed on the SolidWorks models for two separate blade designs (II & III); NACA0021 foil profile first with 0.5 solidity and then with 0.25 solidity. Both have an aspect ratio of 1:1, meaning the diameter and height of the turbine are equal. Through these analyses, we were able to confirm the safety and structural stability of both of these blade designs. This tells us that during testing and regular

performance these blades will succesfully withstand the pressure due to current flow without any drastic changes or failure.

It was decided that these blades would be fabricated via the rapid prototyping machine located in the Engineering building. This machine uses Acrylonitrile butadiene styrene (ABS) plastic, for which the material properties can be found in Table 6 below.

Table 6: Material properties for ABS Plastic

Property	Value	Units
Elastic Modulus	2	GPa
Poisson's Ratio	0.394	N/A
Mass Density	1020	kg/m^3
Tensile Strength	30	MPa
Yield Strength	45	MPa

The blades will be built with fixture plates at either end, which are disks with a diameter of the chord length, and extruded 5mm. Both the NACA0021 blades with solidity of 0.5 and 0.25 respectively, can be seen in Figure 12 below.

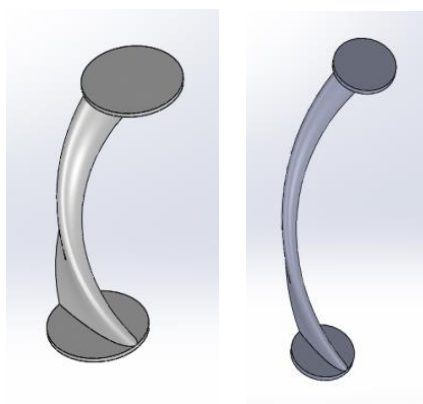

(a) *(b)*

Figure 12: NACA 0021 Blades (a) 0.5 Solidity (Design II) (b) 0.25 Solidity (Design III)

For each analysis, the pressure to which the blades were exposed was varied and the reasoning for each pressure choice is explained in the individual analysis summary below. These analyses are conservative in that they simulate the absolute worst case scenarios that the turbine could be exposed to, and they display how it will behave under these conditions. To ensure a conservative approach, a current speed of 5 m/s was included in CFD, as it is much higher than the design specification of 2 m/s. This subsequently results in a much higher maximum pressure that will be encountered. These pressure values are distributed uniformly across the blade profiles, which also allows for a conservative analysis as the maximum pressure will only occur at one location on the blade as opposed to the entire body. The end plates are fixed for all analyses below, and the exposed pressures are uniformly distributed in one direction which is that of fluid flow.

8.4.1 Aspect Ratio of 1:1, High Solidity Blade Analysis -Design II

For the NACA0021 solidity 0.5 blade, the exposed pressure was a value of 251.325 kPa. This value represents the maximum gauge pressure measured for this blade in CFD analysis when the current speed was 5 m/s (i.e. 150 kPa) added to the atmospheric pressure of 101.325 kPa. This allows for a conservative analysis.

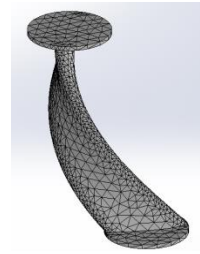

Figure 13: NACA0021 0.5 Solidity Blade Mesh Plot

For this blade, a mesh plot of maximum element size 14.3569mm and minimum element size 2.87137mm was used and is shown in Figure 13. The finer grid allowed for more accurate results and lowered the errors encountered around the sharper edges that result from a coarser grid size.

Both stress and factor of safety profiles were generated from FEA. In Figure 14a it can be seen that a relatively low stress profile is maintained across the entire blade between a range of 0.0832 MPa- 2.59 MPa (the area highlighted in blue) and in some areas a range of approximately 10-20 MPa. The maximum stress that is seen along the model is 30.96 MPa and is found where the blade body meets the fixture pads. It can be seen that the yield strength of the ABS material which was specified to be 45Mpa is never exceeded under the distributed pressure, so we can confirm that the blades will remain structurally intact when exposed to the water current.

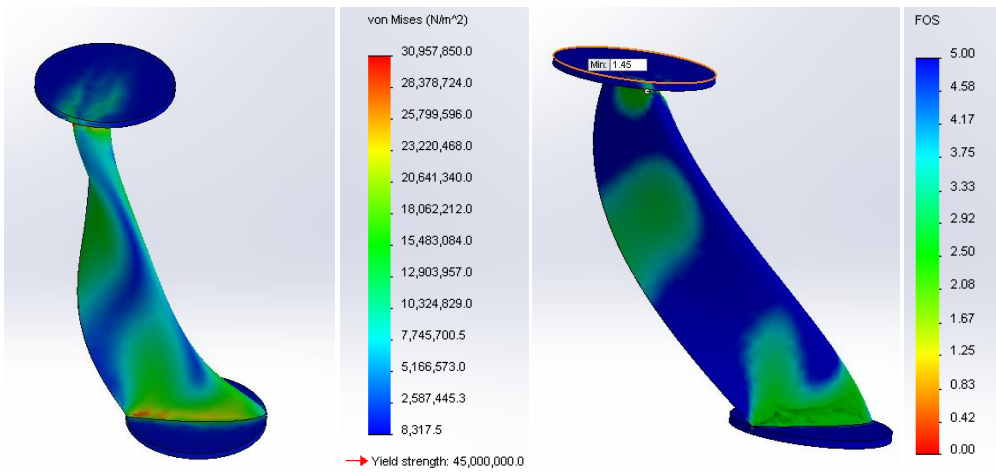

(a) *(b)*

Figure 14: (a) Stress Profile of the NACA0021 0.5 Solidity blade under maximum pressure profile, (b) Factor of Safety Profile of the NACA0021 0.5 Solidity blade under maximum pressure profile (Design II)

The factor of safety varies across the blade profile with values typically greater than 4 (Figure 14b). The lowest factor of safety encountered was 1.45, so this confirms that the blade will not fail while exposed to the specified pressure as the factor of safety is never less than 1.

The lowest factor of safety occurs where the blade body meets the fixture plates. If failure was allowed to occur, the location of failure can be seen in Figure 15 below. This image displays an isoclipping from solidworks that outlines where failure would occur under a safety factor of 2.0.

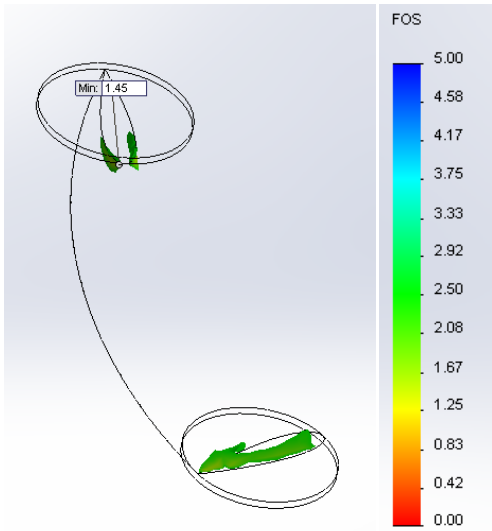

Figure 15: Isoclipping of NACA0021 0.5 Solidity blade displaying failure locations (Design II)

Based on this analysis, we can confirm that the NACA0021 blade with a solidity of 0.5 will not fail during testing and regular performance. This is concluded as there are no locations which exhibit a pressure exceeding yield strength, or a safety factor of less than 1.

8.4.2 Aspect Ratio of 1:1, Low Solidity Blade Analysis - Design III

For the NACA0021,0.25 solidity blade, two analyses were run. First, the exposed pressure was the same value as that of the wider blade used in Design II, (i.e. 251.325kPa). This was to remain conservative during this analysis to determine how the blade reacts under a worst case scenario. A second simulation was run under a lower pressure value of 101.525kPa. These cases are each explained below.

For the blade of 0.25 solidity, both simulations used a mesh plot of maximum element size of 4.63701mm and minimum element size of 0.23185mm (Figure 16).

Figure 16: NACA0021 0.25 Solidity Blade Mesh Plot

Simulation 1: Blade under High Pressure

For the first simulation, the exposed pressure was 251.325kPa. Both stress and factor of safety profiles were generated from FEA. In Figure 17a below, it can be seen that the yield strength of 45MPa is greatly exceeded in the majority of the blade, meaning failure will occur. A maximum stress of 215MPa was seen which would be catastrophic for this blade. This tells us that this pressure value used exceeded the structural capacity for the Design III blade. The larger pressure value is extremely conservative for this blade, as it is the pressure that was achieved in CFD for the Design II blade under a current of 5 m/s.

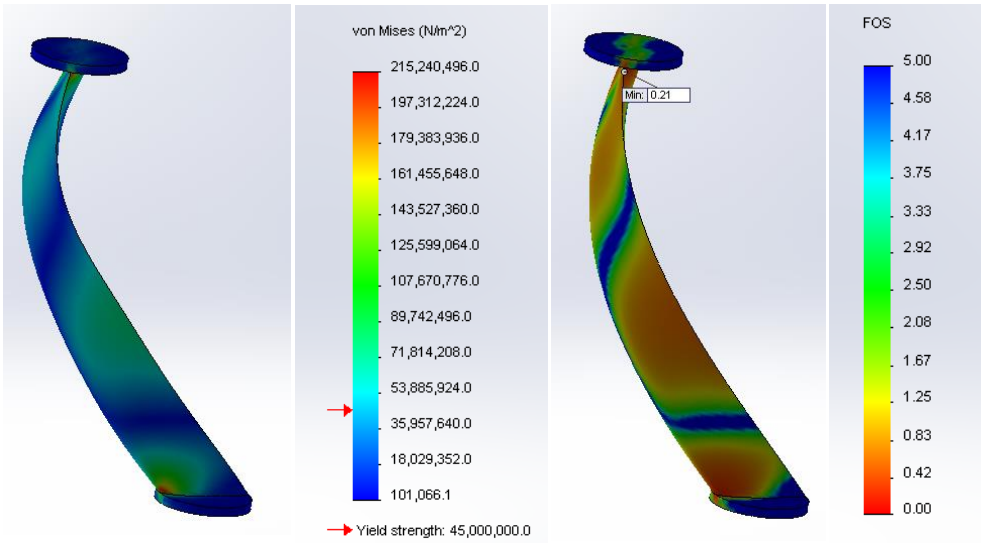

(a) *(b)*

Figure 17: (a) Stress Profile of the NACA0021 0.25 Solidity blade under maximum pressure profile,(b) Factor of Safety Profile of the NACA0021 0.25 Solidity blade under maximum pressure profile (Design III)

Failure is further confirmed when looking at the factor of safety results which are shown in Figure 17b and Figure 18. Figure 17b shows that the lowest factor of safety encountered is 0.21 and occurs in the majority of the blade. A factor of safety below 1 ensures that failure will occur.

Factor of safety values below 1 were exhibted in multiple locations across the blade. Potential locations of failure can be seen in Figure 18 below. This image displays an isoclipping from solidworks that outlines where failure would occur.

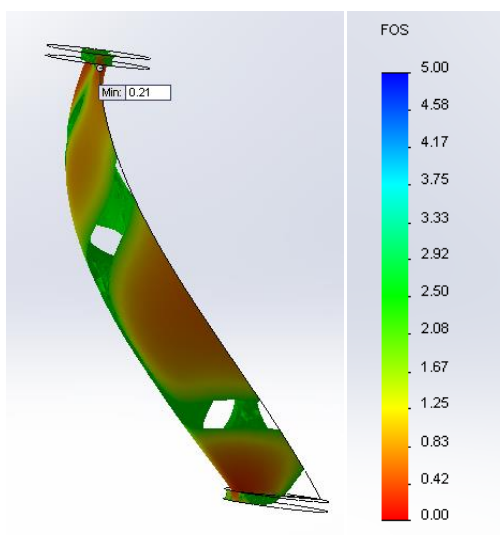

Figure 18: Isoclipping of NACA0021 0.25 Solidity blade displaying failure location (Design III)

Since this analysis exhibited undesirable results using unrepresentative conditions, we decided to run a more realistic scenario for Design III using a pressure of 101.525 kPa as opposed to the large value of 251.325kPa.This scenario and results are described below.

Simulation 2: Blade under Lower Pressure

For the second simulation, the exposed pressure was 101.325kPa. This value is achieved from adding the maximum gauge pressure that was found to be 0.200 kPa for this blade in CFD analysis (when the current speed was 2 m/s) to the atmospheric pressure of 101.325 kPa. This is a lower and more realistic speed that the blade will be exposed to, which should generate more representative and desirable results. The same mesh profile is used in this simulation, and both stress and factor of safety profiles were generated from FEA.

Figure 19a it can be seen that a relatively low stress profile is maintained across the entire blade between a range of 0.02 MPa- 6.75 MPa (the area highlighted in blue) and in some areas a range of approximately 10-27 MPa (the area highlighed in green). The maximum stress that is seen along the model is 40.42 MPa and is found where the blade body meets the fixture plates. It can be seen that the yield strength of the ABS material which was specified to be 45Mpa is never exceeded under the distributed pressure, so we can confirm that the blades will remain structurally intact when exposed to the water current.

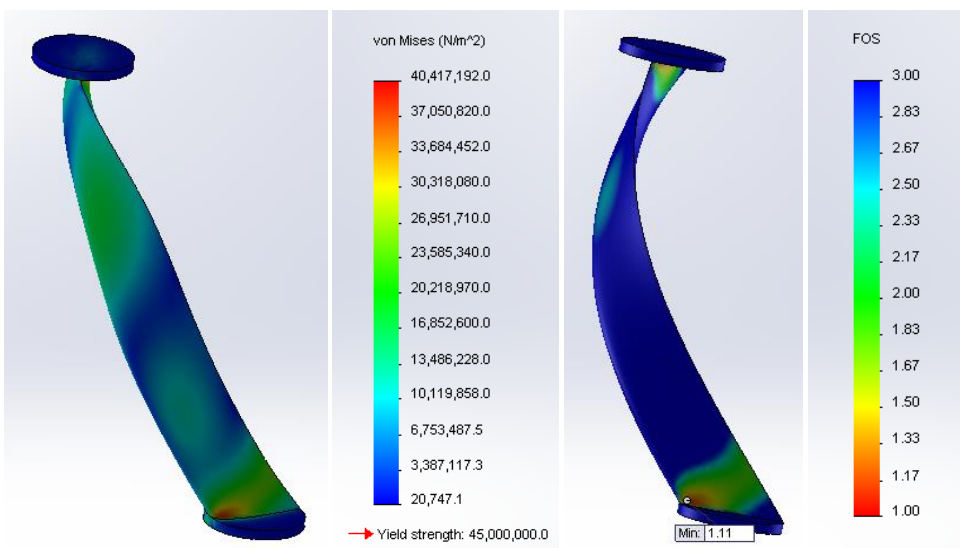

(a) *(b)*

Figure 19: (a) Stress Profile of the NACA0021 0.25 Solidity blade under lower maximum pressure profile, (b) Factor of Safety Profile of the NACA0021 0.25 Solidity blade under lower maximum pressure profile (Design III)

In Figure 19b, it can be seen that the factor of safety varies throughout the blade profile with values typically greater than 3. The lowest factor of safety encountered is 1.11. Although this is relatively low, we can still confirm that the blade will not fail while exposed to the specified pressure as the factor of safety is never less than 1.

The lowest factor of safety is located where the blade body meets the fixture plates. If failure was allowed to occur, the location of failure can be seen in Figure 20 below. This image displays an isoclipping from solidworks that outlines where failure would occur under a safety factor of 2.0.

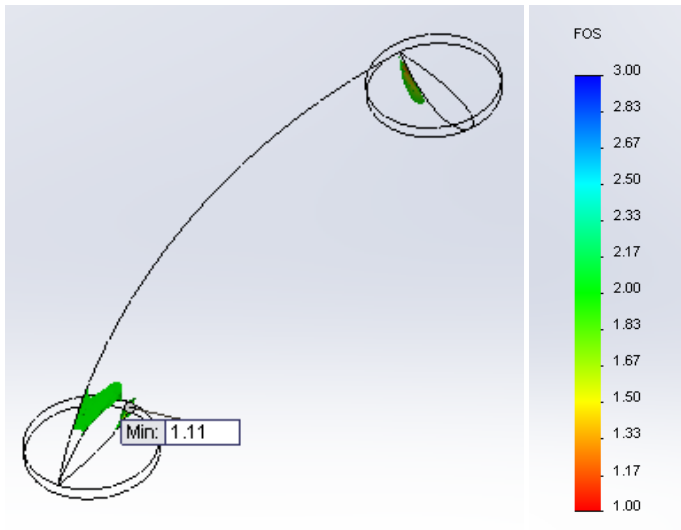

Figure 20: Isoclipping of NACA0021 0.25 Solidity blade displaying failure location under lower maximum pressure profile (Design III)

This analysis exhibited much more desirable results when compared to the first simulation. This is due to using a more realistic pressure as opposed to the absolute worst case scenario pressure that was used for the Design II blade.

From these analyses, we can confirm that neither the NACA0021 blade with a solidity of 0.5 nor the NACA0021 blade with a solidity of 0.25 (Designs II & III) will fail during testing and regular performance. This is concluded as there are no locations which exhibit a pressure exceeding yield strength, or a safety factor of less than 1.

Though the blades clearly withstand the maximum conservative pressures we have applied to them, further FEA analysis is required for the turbines. Most importantly a fatigue analysis will be required for each blade configuration due to the cyclic nature of loading and unloading that the blades and turbine as a whole will experience. This analysis will be completed in the final phase of the design.

8.4.3 Fatigue Analysis

In addition to FEA, a fatigue analysis was ran on both blades in SolidWorks to determine if they would survive an infinite life. The results are outlined for NACA0021 with 0.5 solidity (Design II) and NACA 0021 with 0.25 solidity (Design III) in

Figure 21a and Figure 21b below, respectively. The areas highlighted in blue are the areas which will survive an infinite life, while the areas highlighted in red will not survive.

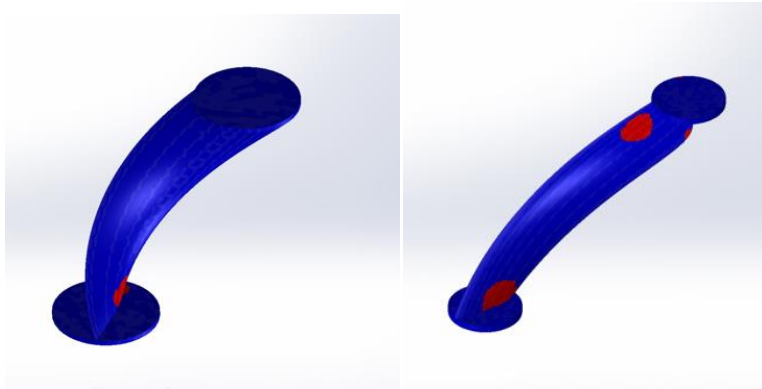

(a) *(b)*

Figure 21:Solidity fatigue check for blade designs II & III (a) NACA0021 with 0.5 Solidity Fatigue Check, (b) NACA0021 with 0.25 Solidity Fatigue Check

It can be noted from Figure 21a above that the discontinuity area where the blade meets the mounting plates will fail and not achieve infinite life. This further confirms the results that were obtained in FEA.

It can be noted in Figure 21b above that the blade with lower solidity will fail in multiple areas and have a finite life. These results are as expected as the highest regions on the von-mises stress plot align with the suspect areas on the fatigue checks. This makes sense as they are not in the center of the blade, but rather at or near the ends, where the cross section changes and stress concentrators are present.

8.5 Blade Mount Design

Turbine blades will be screw-mounted to two pre-drilled aluminum end plates with an epoxy-bonded layer, or poured resin for smoothing and reinforcement. One end plate and associated epoxy-bounded layer is shown in Figure 22. The turbine shaft will penetrate through the turbine for added rigidity, but if initial testing is not successful, it will then be affixed to only one plate so as to investigate the performance of the turbine without interior shaft interference. This arrangement allows for ease of initial attachment and positioning of blades, and allows for quick replacement in the event of blade failure.

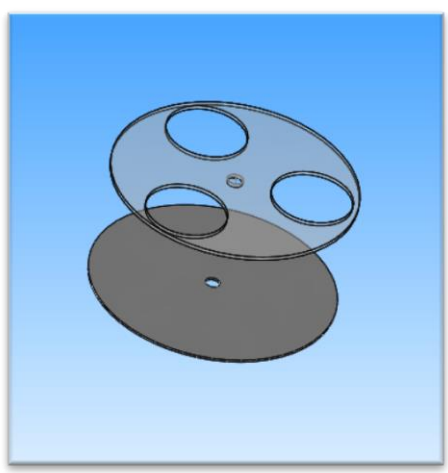

Figure 22: Blade Mount Design

8.6 Detailed Design Summary

In Summary, the team designed three turbines, as shown below in Figure 23, to be fabricated and tested;

- Turbine Design I – NACA 0018, 0.3 Solidity Blades
- Turbine Design II – NACA 0021, 0.5 Solidity Blades
- Turbine Design III – NACA 0021, 0.25 Solidity Blades

The endplates for each turbine follow the same design; where turbine blades are to be screw-mounted to two pre-drilled aluminum end plates with an epoxy-bonded layer, or poured resin for smoothing and reinforcement.

Turbine Design I contains the preliminary blade design. Using CFD, this design was optimized and Turbine Design II (NACA 0021, 0.5 solidity blades) was chosen for fabrication. Turbine Design II was identified to have optimal self-starting capabilities. We chose to fabricate Turbine Design III, a turbine of identical foil and chord length to Turbine Design II with half the solidity, 0.25.

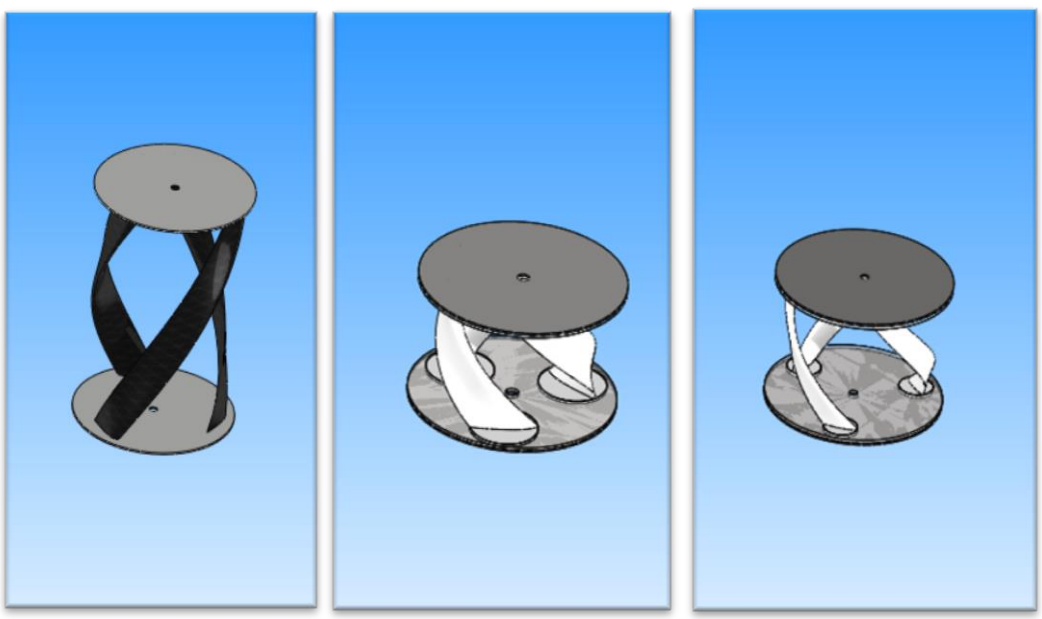

(a) *(b)* *(c)*

Figure 23: Detailed Turbine Designs (a) Turbine Design I (NACA 0018, 0.3 Solidity), (b) Turbine Design II (NACA 0021, 0.5 Solidity), (c) Turbine Design III (NACA 0021, 0.25 Solidity)

9 Fabrication & Testing

The fabrication and testing phase outlines how the designed turbine blades and endplates were fabricated, the assembly of turbines II and III as well as the testing of turbines II and III in Memorial University's wave/tow tank and wind tunnel. A discussion of testing results follows.

9.1 Fabrication of Blades

The turbine blades were fabricated using two different methods. Turbine design I blades were fabricated by DJ Composites Inc. using composite materials, as shown in Figure 24a. Turbine designs II and III blades were fabricated using Memorial University's rapid prototyping machine with ABS plastic as material, as shown in Figure 24b and Figure 24c respectively.

(a) *(b)* *(c)*

Figure 24: Fabrication of Blades (a) Blade Design I (NACA 0018, 0.3 Solidity), (b) Blade Design II (NACA 0021, 0.5 Solidity), (c) Blade Design III (NACA 0021, 0.25 Solidity)

9.1.1 Composite Blade Fabrication -Blade Design I

Composite blade fabrication and design was completed by DJ Composites Inc. The composite blades were fabricated for the Design I turbine; 1:2 aspect ratio turbine using the NACA 0018 foil shape with a solidity of 0.3 and an angle of attack of 9 degrees. The fabrication goals for this turbine were to have a high strength to weight ratio, good surface finish and minimal cost.

DJ Composites is a company located in Gander, Newfoundland that specializes in composites specifically for use in aircraft (e.g. fuselages). They utilize high-end composites and have a 6-axis CNC machine capable of producing complex shapes which is ideal for our application of helical blades.

The fabrication process started with the proper file extension (.iges), exported from the SolidWorks model. DJ composites Inc. then created identical shells (half of the foil shape each) using a CNC machine. The material used was Renshape 5008, as shown in Figure 25, which is an epoxy with a low coefficient of thermal expansion for use in autoclave curing. This material can withstand the high temperatures in an autoclave and gives excellent surface properties to the composites being cured.

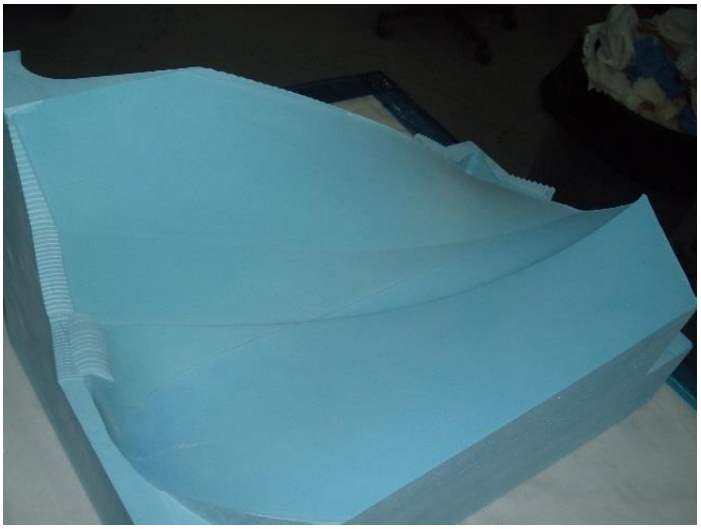

Figure 25: Renshape Fabrication Foam

The composite blades have two layers of woven graphite on the outermost layer. The internal structure consists of foam inserts which are located at the thickest part of the blade. The tip and tail of the foil are filled with a potting material. The foam provides flexural rigidity while the potting material fills the other voids and resists physical shock and vibration. At the tip, tail and foam interface, aircraft grade adhesive connects the two half-blades, completing the helical blade design. Furthermore, a stronger resin is incorporated at the top and bottom of the completed blade to allow for stronger fixture properties when connected to the end plates. A detailed drawing of the blade cross section and materials is located in Appendix D.

9.1.2 Rapid Prototyped Blade Fabrication - Blade Designs II & III -

Design II (NACA 0021, 0.5 Solidity) and Design III (NACA 0021, 0.25 Solidity) turbine blades were fabricated using Memorial University's rapid prototyping machine as shown below in Figure 26.

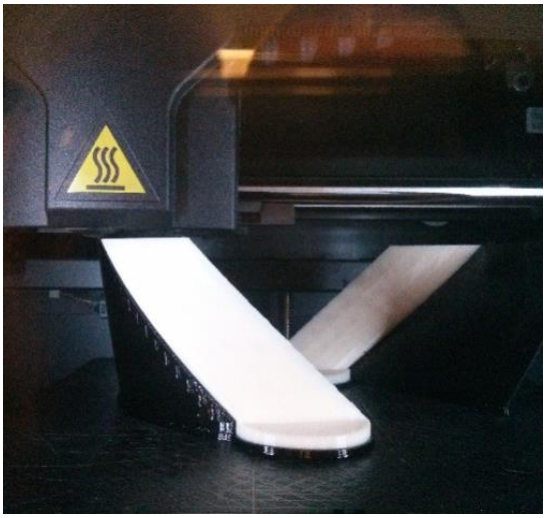

Figure 26: Rapid prototyped Blades midway through fabrication

A .stl file was first exported from the SolidWorks model as this is the file type required by the rapid prototyper. Both turbines used the same material, ABS M30, and were rapid prototyped using the faculty's resources. Each blade took on average 8 hours to complete in the prototyper and were designed with mounting plates at each end of the blade to allow for easier mounting to the turbine's end plates. The speed of prototyping allowed for fabrication and testing of two foil shapes and aspect ratios. Roughness of blades, resulting from this fabrication will induce turbulent boundary layer, which is desirable at low Reynolds numbers to delay flow separation and increase effectiveness of foils (increase lift). Many wind turbines utilize vortex generators to delay boundary layer detachment (24). This effect is shown in Figure 27.

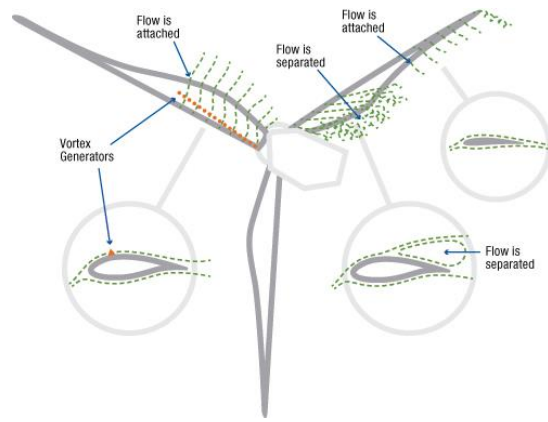

Figure 27: Effect of Boundary Layer Flow (26)

9.2 Fabrication of End Plates

Turbine blade mounts were chosen to be designed as endplates, as shown below in Figure 28, rather than spokes. The endplates allowed for the easiest prototype fabrication, and the least build and set-up time. Endplates were composed of two layers: an outer aluminum circle of 3mm (1/8 inch) aluminum plate, with an inner 6mm layer of acrylic. The inner acrylic layer had recesses spaced at 120° which were laser-cut to fit the blade mounting plates. Holes were drilled and tapped through both layers while they were clamped in place. The layers were then fastened together with ¼"-20 x3/8" screws. Additionally, an aluminum collar was bolted through the aluminum and acrylic, "sandwiching" the plastic between two aluminum components. The aluminum collars also had three set screws, offset by 120°, for friction-fitting the turbine to the shaft to prevent rotation and slippage.

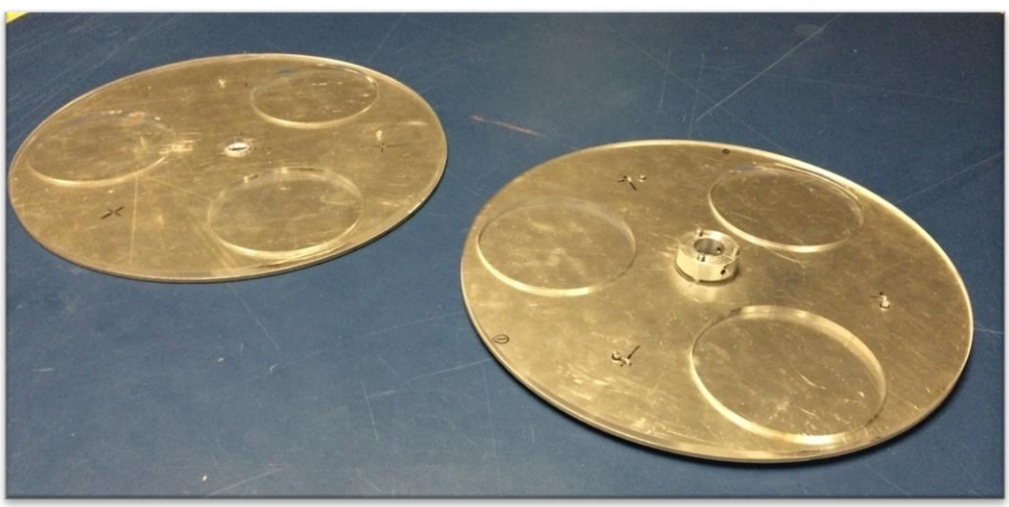

Figure 28: Turbine II End Plates

9.3 Assembly of Turbines

Turbine Design II (NACA 0021, 0.5 Solidity blades) and Turbine Design III (NACA 0021, 0.25 Solidity blades), as shown in Figure 29b and 29c respectively, were assembled for testing. Due to time constraints, Turbine Design I (NACA 0018, 0.3 Solidity) was not assembled. Figure 29a shows Turbine Design I simply fixed together using tape purely for visualization purposes.

For the assembly of Turbines II and III, one endplate was mounted on the appropriate shaft, and the blades were individually clamped in place to it. The second endplate was then fit onto the shaft, but not set in place, and the blades were adjusted to fit into the recesses in the acrylic. Once blade mounting pads were aligned in recesses in both endplates, the second endplate was then friction fit to the shaft by tightening the set screws. The blades, which were now "sandwiched" between both endplates, were clamped to each endplate on each end (for a total of 6 clamps). The aluminum endplates and mounting pads of the blades were then drilled and tapped in place, while clamped. After cleaning, the blades were then fixed to the endplates using 10-24x3/8" machine screws.

Turbine Design II was chosen to be tested in Memorial University's wave/tow tank and will be referred to as the water turbine. Turbine Design III was chosen to be tested in Memorial University's wind tunnel and will be referred to as the wind turbine.

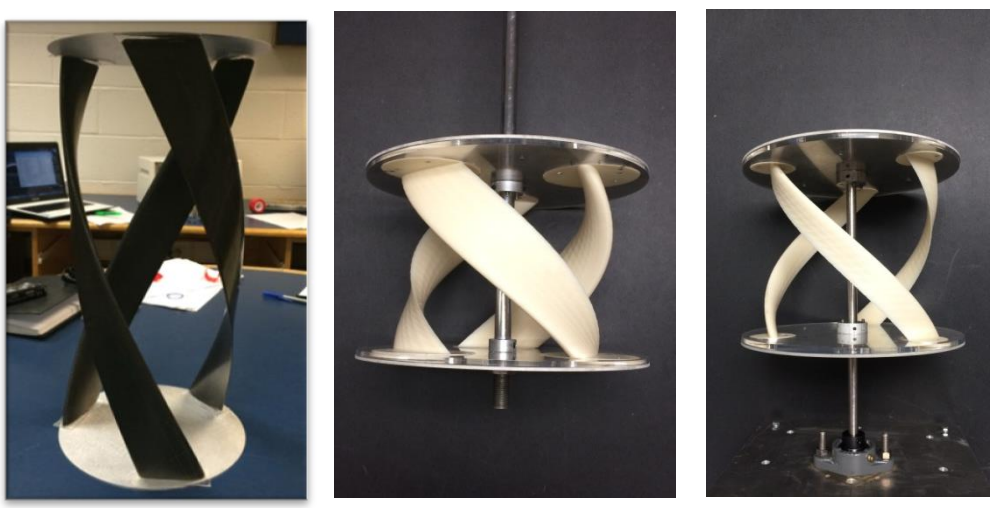

(a) *(b)* *(c)*

Figure 29: Assembly of turbines (a) Turbine I (NACA 0018, 0.3 Solidity)* simply fixed with tape for visualization, (b) Water Turbine (NACA 0021, 0.5 Solidity), (c) Wind Turbine (NACA 0021, 0.25 Solidity)*

9.4 Testing Frame Fabrication

Two testing frames were fabricated for testing of the water and wind turbines. The water turbine required a custom test frame for testing in Memorial University's wave/tow tank. The wind turbine required a custom test frame for testing in Memorial University's wind tunnel.

9.4.1 Wave / Tow Tank Testing Frame –Water Turbine

For cost and materials savings, the wave/tow tank test frame, as shown below in Figure 30, was re-manufactured to fit a shaft size appropriate for the tested turbine. To accomplish this fit, linear bearings

were removed from the bearing support tube, and the tube was re-machined to fit two ¾"ID deep-groove bearings. Deep groove bearings were specified to carry the light axial load from the weight of the turbine and shaft assembly. The vertical position of the shaft was maintained through the use of collars, held in place by set screws, with the upper collar having a shoulder to sit only on the inner race of the bearing, and an overall outer dimension equal to the bearing support tube, to prevent fall-through in the event of bearing failure. The bearing support tube was re-fit into the unmodified test frame mount, which was then bolted to the standard test frame for the wave/tow tank carriage.

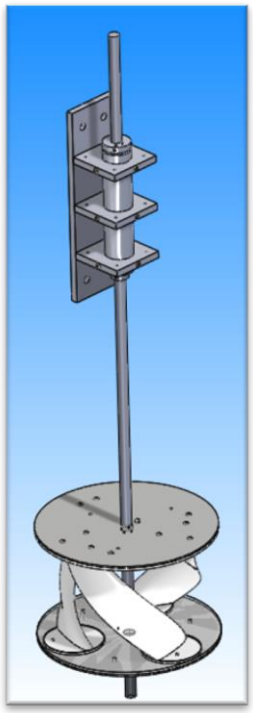

(a)

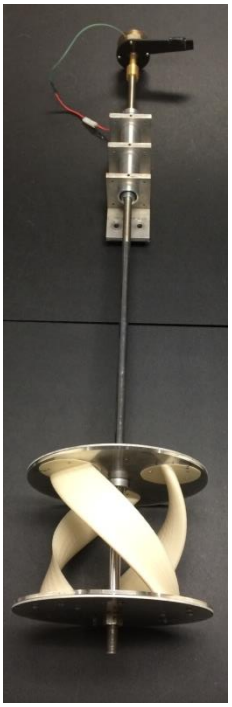

(b)

Figure 30: Tow Tank Testing Frame (a) Solidworks model, (b) Fabricated wave/tow tank frame

9.4.2 Wind Tunnel Testing Frame –Wind Turbine

Similarly, the wind tunnel test frame, as shown below in Figure 31, was re-used from a previous experiment. In this instance, however, little modification was required since the turbine shaft diameter remained the same. The mount consists of two aluminum plates, separated by four 100mm long aluminum rod spacers, tapped for bolting of plates to each end. These spacers were shortened to 100mm from 150mm to allow the shaft to reach through the tunnel floor. A flanged bearing is bolted to the center of each plate, and the shaft passes through each bearing, and through each plate. This enables the shaft to fit through a penetration in the wind tunnel floor so torque and power measurements can be taken from the shaft externally.

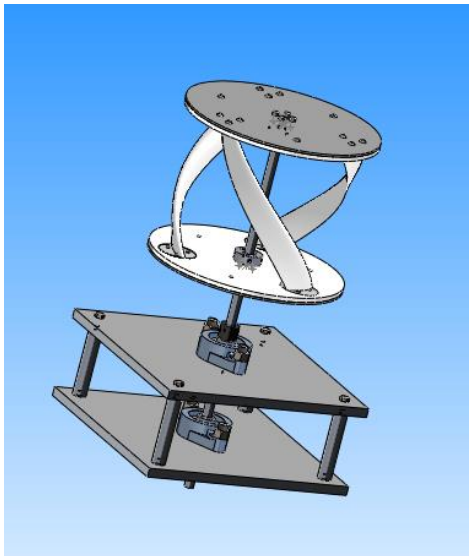

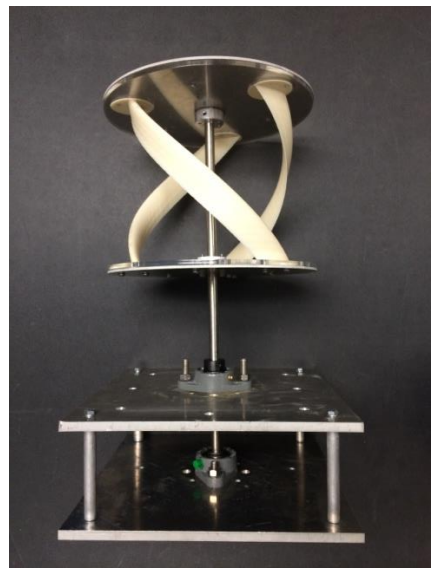

(a) *(b)*

Figure 31: Wind tunnel testing frame (a) Solidworks model, (b) Fabricated wind tunnel frame

10 Prototype Testing

Water and wind turbine test set up, methodology and results are explained in this section.

10.1 Testing Motivation

The objective of our scale model testing was to demonstrate power generation.

10.2 Water Turbine Testing

The water turbine (NACA 0021, 0.5 Solidity) was tested in the wave/tow tank at Memorial University. Key measurements recorded were the starting torque of the turbine and the maximum no load rotational speed. Our team has salvaged a previously fabricated test frame as described previously in section 9.4 of this report. There is an existing data acquisition system equipped with LabView attached to the towing carriage. We used the existing set-up in addition to a magnetic torque brake to record our measurements.

10.2.1 Test Set-up

Testing the designed and built turbine is the final step in validating the model. Closing the loop of engineering, the results must be compared to what was predicted with theory. For the water turbine (NACA 0021 with 0.5 Solidity), a decision was made to test in the wave/tow tank as shown below in Figure 32. Though other facilities are available for use in the fluids laboratory, particularly the flume tank, the towing capability (maximum carriage speed of 5 m/s) of the wave/tow tank coupled with the overall size of the tank was attractive test parameters. The flume tank simply was too small to accurately test the turbine, as wall effects would have been too evident.

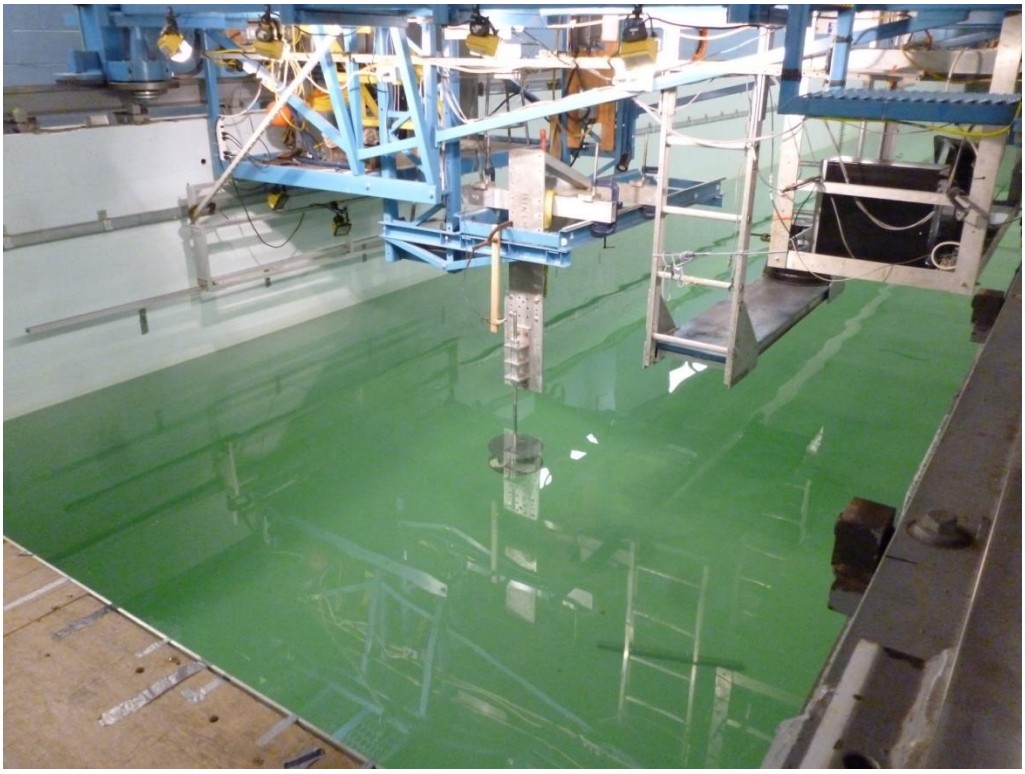

Figure 32: MUN Wave/Tow Tank

At 52 m long, 5 m wide and 3 m deep, the wave/tow tank would provide enough distance from walls to accurately test the turbine. Also, at 3 m deep, the turbine could be mounted well below the surface of the water to minimize or eliminate cavitation effects. The length of the tank also allowed the turbine to easily reach steady state such that measurement of the testing results was easy.

The test setup consisted of a large aluminum frame which was salvaged as described above in section 9.4. The frame was clamped to support bars on the towing apparatus. Attached to the apparatus is a bracket which houses the bearing used and was modified specifically for the experiment. A safety collar was attached to the ¾ " shaft which allowed the shaft to rotate about the inner race of the bearing. Also, the safety collar was wider above where the bearing sits to allow for the turbine setup to remain intact should the bearing fail.

For testing, the turbine was attached to the shaft and submerged in the water approximately 0.6 m from the surface of the water to the top endplate. An optical tachometer was clamped to the towing carriage and centered such that a reading on the shaft was made. Reflective tape was attached to the shaft to increase its reflection and aid on the data acquisition (DAQ). Optical tachometers read rotational speed, a key component in our testing.

A magnetic brake, complete with a ½" to ¾" adapter was used for the test. This brake was mounted using the adapter, to the top of the shaft. A moment arm on the brake allowed for it to rest against the test frame and apply the necessary torque. The B35 12-volt brake by placid industries (See Appendix F for brake specifications) was connected to a power source so that the current could be varied. The relationship of current input to brake torque is correlated and displayed graphically on the brake specification sheet.

The towing carriage is capable of towing at fixed or variable speeds. The speed is controlled by the user and input into the DAQ system as a voltage. The towing capabilities of the carriage allow for variable speeds up to 5m/s, well above our turbine design. The carriage speed is what simulated flow speed due to relative motion were all recorded. For each of these runs, the RPM was recorded such that power could be calculated. Figure 33 below illustrates the key components of the test set-up in the wave/tow Tank.

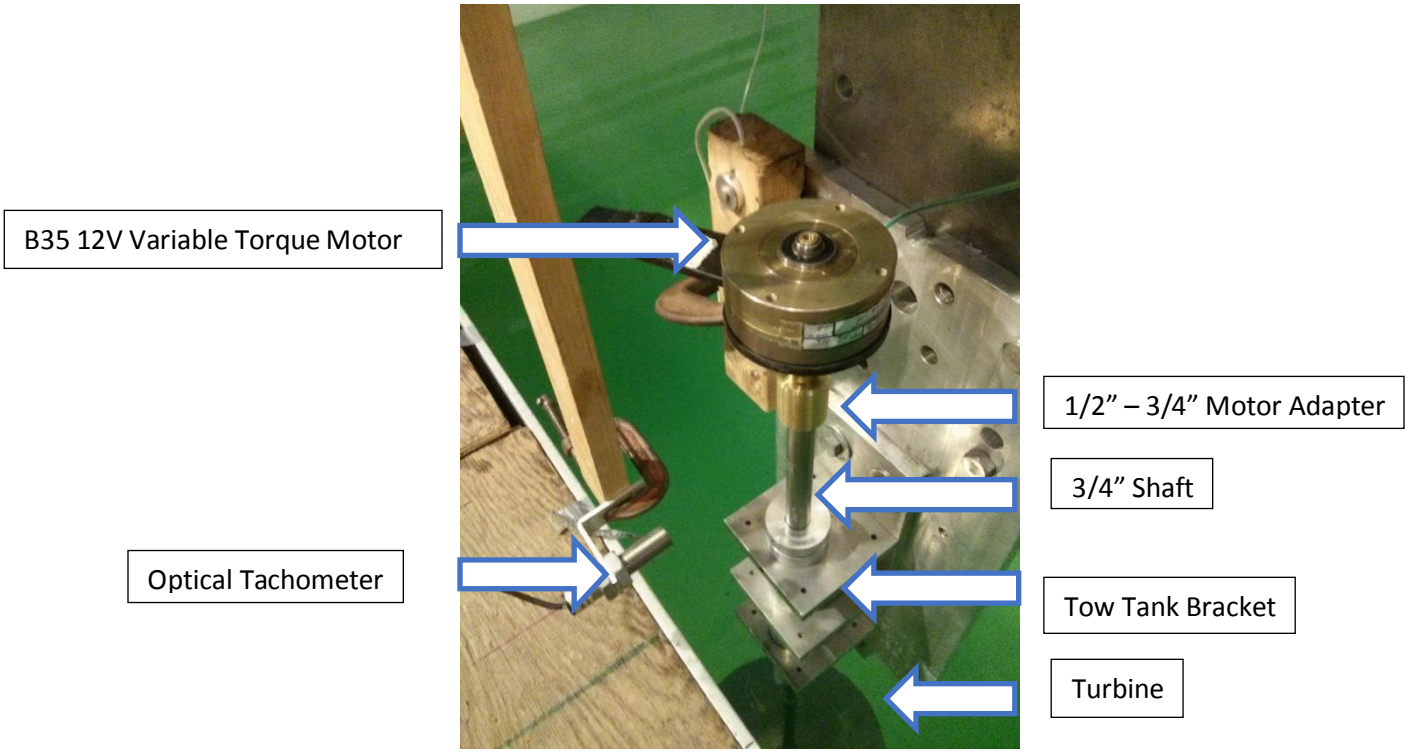

Figure 33: Wave Tow Tank Test Set-up

10.2.2 Test Methodology

The water turbine (NACA 0021, solidity 0.5) was fixed to the wave/tow tank carriage to be pulled through the water at a fixed speed. The testing was completed at intervals of 0.25 m/s from 0.25 m/s to 2 m/s. This was to simulate various flow speeds and also determine at what speed(s) the turbine performed the best. This best operating point is coincident with a specific speed coefficient, which relates the tangential velocity of the blades to the water flow speed.

Initially, the turbine was towed through the tank at each speed, to reach steady state and provide its steady state RPM. This initial speed was induced without the brake connected so that the freewheel RPM could be determined – a key component in turbine and turbomachinery theory.

Next, the brake was attached to the shaft to allow the application of brake torques. At each speed interval, torque was increased by gradually increasing the current applied to the brake. This was continued until a stalling brake torque was determined. Once determined, equal intervals of torque were applied for test runs at each speed level. This allowed for a full power curve to be developed as values of zero torque (freewheel RPM), full stall torque (zero RPM) and several torque values between were all recorded. For each of these runs, the RPM was recorded such that power could be calculated.

10.2.3 Data Acquisition System

Another key component of the wave tow tank is the integration of a DAQ system. Information from the test is read by the DAQ system and displayed/output as a value specified by the user. Namely, voltage values are read by the DAQ system and correlated with a user-defined relationship to output data in the correct units. DAQ allows better control and accurate results for such tests and saves a lot of time vs. comparable manual setups (e.g. pony brake with a manual variable torque).

National Instruments is the manufacturer of the DAQ system apparatus and software. Specifically, the software used was LabView Signal Express. As previously mentioned, voltage from various sources (optical tachometer, chassis speed controller, motor torque, and time) were measured, recorded in the DAQ and correlated into usable data. The test used units of Newton-meters (N-m) for torque, seconds (s) for time, meters per second (m/s) for carriage speed, and revolutions per second (RPS) for angular speed. Also, displayed on the carriage, was output from the optical tachometer in RPM.

10.2.4 Testing Results & Discussion

Each set of test data logged hundreds of thousands of data points. By analyzing the data, the steady-state point was observed and data was averaged after that point. Again, the key data was motor torque, carriage speed, and rotational speed. The following is the actual final averaged test data. The data was averaged because too many data points are not desirable for analysis.

This power data was plotted vs. rotational speed, as shown below in Figure 34. Power curves were generated for each tested flow speed. A general trend is observed following the well-known turbomachinery laws regarding power and RPM. It can be seen that our turbine output 13 W of power at 2m/s flow speed. The curve also generally confirms our previous preliminary testing assumption that maximum power occurs at approximately half of the freewheel RPM.

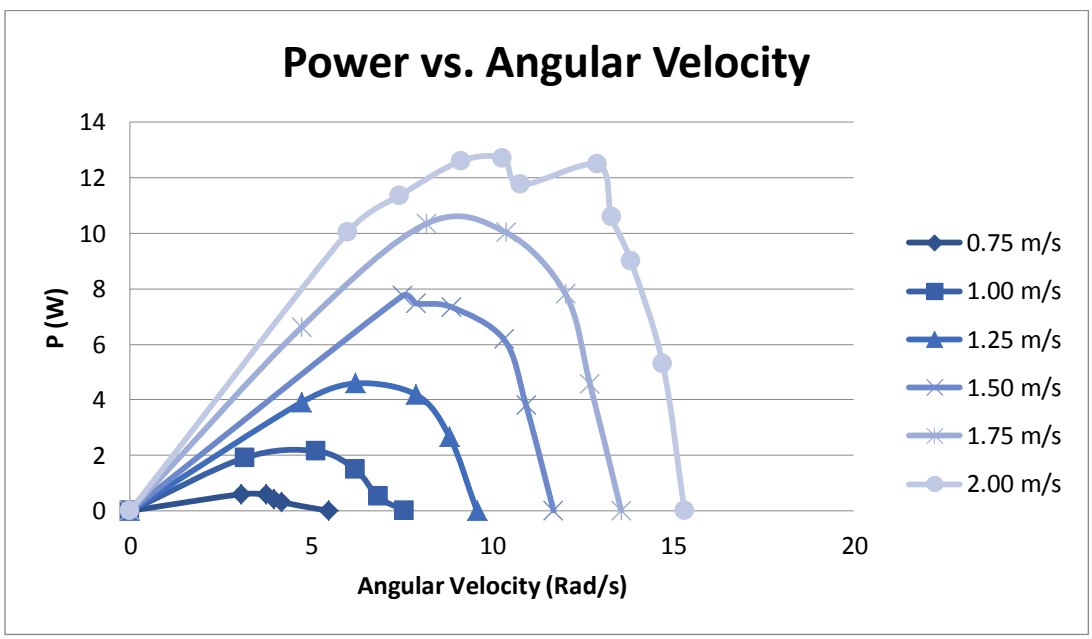

Figure 34: Power vs. Angular Velocity (Water Turbine)

Another parameter of a turbine is its non-dimensional performance. A performance curve follows and is specific to the turbine prototype. Non-dimensional power and speed are plotted against each other to show optimal turbine performance. Non-dimensional power is C_p, non-dimensional speed is C_s and is sometimes referred to as tip-speed ratio. Calculation of these parameters is shown in Equations 5 and 6 below.

Equation 5: Turbine performance Equation

$$C_p = \frac{P}{\frac{1}{2}\rho A U^3}$$

Where:

$C_p = Coefficient\ of\ turbine\ performance$

$P = power\ generation\ (Watts)$

$\rho\ = fluid\ density\ ({}^{kg}/_{m^3})$

$A = cross\ sectional\ area\ of\ turbine\ (m^3)$

$U = fluid\ stream\ speed\ ({}^{m}/_{s})$

Equation 6: Turbine Speed Equation

$$C_s = \frac{R\omega}{U}$$

Where:

$C_s =\ Coefficient\ of\ turbine\ speed$

$\omega\ =\ angular\ velocity\ ({}^{rad}/_{s}$

$U = fluid\ stream\ speed\ ({}^{m}/_{s})$

$R\ =\ turbine\ radius$

When plotted, this performance curve basically shows the efficiency of the turbine. As seen in Figure 35 below, the maximum efficiency is approximately 12% (ratio of power extracted to theoretical available power in the fluid) for the 1.25 m/s flow speed at a C_s of approximately 1. This means that in general, when the tangential speed of the blades is equal to the speed of flow, power is maximized.

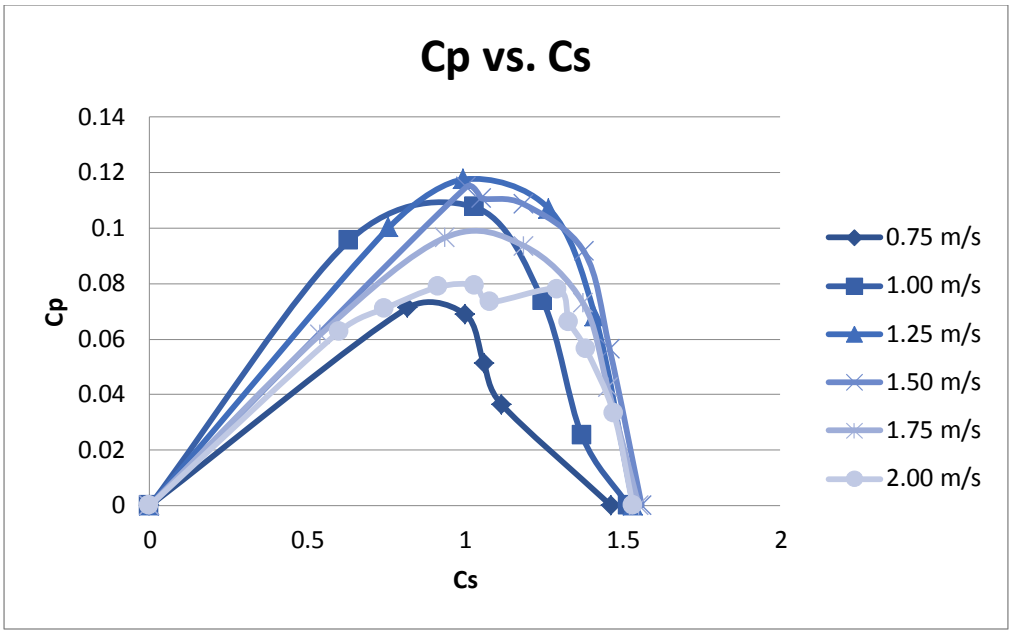

Figure 35: Coefficient of power vs. coefficient of turbine speed (Water Turbine)

The values observed here for C_p vs. C_s are lower than what research literature has indicated. As mentioned previously, Gorlov helical turbines can obtain efficiencies up to about 35%. With optimized design through Design of Experiments (DOE), ideal materials (composites), and more efficient coupling/connections, it is believed that C_p values greater than 12% are attainable but currently beyond the scope of the project.

10.3 Wind Turbine Testing

The wind turbine (NACA 0021, 0.25 Solidity) was tested using Memorial University's wind tunnel.

10.3.1 Test Set-up & Methodology

The wind tunnel is a horizontal open-circuit facility with a rectangular 20.0 x 0.93 x 1.04 meter test section, as shown in Figure 36 below. The key measurement recorded was the maximum no load rotational speed. Our team has salvaged a previously fabricated test frame as described previously in section 9.4 of this report. A handheld tachometer was used to measure rotational speed of the turbine and a hot wire anemometer was used to measure wind speed.

Figure 36: MUN Wind Tunnel

10.3.2 Testing Results & Discussion

We chose to test the wind turbine in the wind tunnel to investigate the self-staring capabilities of the helical turbine in a low density fluid stream. While the water turbine performed better than expected, there were some difficulties with the lower-solidity turbine testing in the wind tunnel. The first test run of the turbine actually failed to achieve self-starting at a maximum wind speed of approximately 14.5 m/s. The decision was made to replace the test mount bearings, which we felt were worn, poorly lubricated, and as a result had a high resistance to shaft rotation. The bearings were replaced like-for-like, due to time constraints for testing. With the replacement bearings, and a slight modification of the wind tunnel to increase flow speed, the turbine achieved self-starting at a wind speed of 15.7 m/s. After self-starting at this wind speed, the turbine achieved a steady state RPM of 132, equating to a TSR of approximately 0.18 (notably much lower than the turbine tested in water). The decision was made to not take torque readings from the current wind tunnel test setup as we didn't have an accurate method of applying amounts of brake torque small enough to allow the shaft to continue rotating, especially with the inefficient bearings. The acquisition of a properly sized brake or generator to allow proper testing for the third turbine is outlined in the section 14 Future Work. The modified setup is shown in Figure 37 below.

Figure 37: Modified Wind Tunnel Test Set-up

10.4 Discussion of Error

While every effort was made to ensure data gathered was as accurate as possible, some sources of possible error have been identified for both the water turbine tests in the wave/tow tank and the wind turbine tests in the wind tunnel.

For the water turbine testing, during 1.75 m/s and 2.0 m/s tow tests, it was noticed that the ¾" shaft for the water turbine began oscillating, causing the turbine at the end of the shaft to orbit the original neutral position. This would likely have some effect on both the torque output of the turbine, as well as the angular velocity of the rotor and shaft. Additionally, as the power supply used was analog in adjustment and display, an in-line multimeter was added to the power supply setup for the magnetic brake to give a more accurate current reading. The addition of this in-line resistance may have had some effect on the current supplied to the magnetic brake, and therefore the braking torque. Error may have been introduced depending on the calibration of other equipment used: carriage speed sensor, optical angular velocity sensor, and magnetic brake. Additionally, we were unable to determine mechanical losses in the turbine shaft mount bearings due to not having equipment sensitive enough available.

For the wind turbine testing, the main source of error occurs due to the bearings on the wind turbine mount. These bearings are not efficient enough to make testing for torque practical, since there is too much power loss in the mechanical resistance of the bearings.

10.5 Lessons Learned

The following are the main lessons learned from turbine testing and the required actions to improve testing equipment and results.

1. Magnetic brake: The magnetic brake used was very effective, and definitely saved time in both data collection and analysis, but due to torque rating, was a little too powerful at its lowest end for the speeds at which we wished to test the turbine. Ideally, a properly specified magnetic brake, torque transducer, or dynamometer (generator used to determine torque) would be used, allowing the gathering of more complete data, especially from the wind tunnel, where less torque seems to be generated overall.

2. Power Supply: More accurate power supply is needed for use with the magnetic brake. As current is increased at a constant voltage, the brake applies more resistance to turning (torque) to the shaft. Unfortunately, the power supply used was an older analog version, which made fine adjustments to current difficult. Since current values varied between 0 and 0.67A, a rather small range, this made getting small increases in torque for each trial run rather exacting.

3. Shaft and support: The shaft used for testing the water turbine was smaller than the shaft originally paired with the turbine mount (3/4" as compared to 1"). While this was an appropriate size for the turbine, and the mount was properly re-machined to fit, the thinner (and less rigid) shaft began to show visible oscillation due to the overall drag of the turbine as stream speeds approached 2 m/s. Ideally, the bearing housing would be extended to near the water surface, to increase support for the shaft and allow the testing of higher flow speeds. This is actually quite simple, and likely reasonably inexpensive to fix: simply machine a slightly longer aluminum tube (current bearing housing is cut from aluminum tube standard stock) to fit the current bearing setup.

11 Risk Analysis

There are numerous risks associated with hydroelectric generation. These risks appear in the forms of, but are not limited to, environmental, safety, maintenance, legal, and ecological. Without appropriate planning and identification of risks associated with a project, hazards can occur from the lowest to highest of scales. The following are some of the potential risks expected to be associated.

Loss of aquatic life is a major risk for free-stream energy generation. It is clear that a turbine placed in a waterway can have disastrous effects primarily to marine life as well as the accompanied damage to the system. As well it would render the project non-feasible if the cost of repair or downtime decreases the effective efficiency (e.g. it may no longer be economically viable to re-build the system after failure).

There is also a potential hazard to human life due to the nature of spinning blades. This should not pose a large problem for such a small scale project but it still needs to be considered.

With any hydroelectric generation project there involves risk of electric shock in the waterway. This would cause major problems to the adjacent marine flora and also any animals that come within range to be affected.

Failure of machinery risks are of major importance as well as they can make or break a project. If there is too high a probability of catastrophic failure risk then the system will have to be redesigned. In this phase of the project we have spent a considerable amount of time designing our turbine to mitigate this risk. Our FEA analysis has resulted in the determination of safe limiting flow speeds for the NACA 0021, 0.5 solidity turbine which is 5 m/s and the NACA 0021, 0.25 solidity turbine which is 2 m/s. A fatigue analysis has also been conducted. These analyses have mitigated risks affecting the structural integrity of the turbines. These risks can also include sustained corrosion or damage to the blades or rotor due to sediment travel in a river. As we are not sure that maintenance-free mechanical equipment exists, we propose a low-maintenance design that allows waterproofing of system components. A magnetic couple would allow the transfer shaft to be linked from the turbine, to the interior of a waterproof housing with no mechanical penetrations or seals. We believe this technology, in use for underwater vehicle drives, is adaptable to the environments predicted for this type of turbine installation.

There is regulatory risk as well due to the waterways proposed for application being public. Permission and approval by government is a requirement for such projects as they will modify existing public spaces and ultimately the public has a large voice as to whether approval will be met.

The Power Rangers Team minimized risks during wave/tow tank testing by adhering to Memorial University's Safety Policies. A personal floatation device was worn by team members while performing testing in the wave/tow tank and special care was taken when the towing carriage was in motion.

12 Economic Analysis

The final budget for this project can be seen in Table 7 below. We were allotted $250.00 provided from the faculty and each team member has also contributed $50.00 to the project . In addition, our team has solicited $500.00 of funding from Nalcor Energy to aid us in achieving our fabrication targets. Combining the three finance sources gives us a total budget of $1000.

A major cost to this project was the manufacturing of six ABS plastic helical blades. We cut done on costs by salvaging parts from previous turbine design projects. Our largest cost savings from salvage comes from the tow tank mount, and the wind tunnel test frame, both of which we modified to fit our turbines. Materials cost savings for both is estimated to be approximately $1,000, with labour costs undetermined. The bulk of this savings comes from the tow tank mounting frame. Our composite blades were donated by DJ Composites Inc.; this has also caused a major reduction to our budget.

Table 7: Project Budget

Budget			
Materials Purchased	Cost ($)	Quantity	Full Cost ($)
Aluminum End Plates	17.50	4	70.00
Acrylic Material for End Plates	37.50	2	75.00
ABS Plastic Helical Design II Blades (Rapid Prototype)	163.30	3	489.90
ABS Plastic Helical Design III Blades (Rapid Prototype)	50.90	3	152.70
Composite Helical Blade (DJ Composites)	0 (Donated)	3	0.00
Mounting Frame (Aluminum materials)	0 (Salvaged)	1	0.00
Wind Turbine Bearings	12.00	2	24.00
Water Turbine Bearings	6.50	2	13.00
Collars	4.50	4	18.00
Fastening Hardware	30.00	1	30.00
Reports	30.00	3	90.00
Total			$962.60

The total cost of our three turbines was $962.60. We successfully fabricated and tested our turbines below our budget of $1000.

General information on scale economics of producing a full-sized turbine installation would not be accurate, since each installation would have to be customized to suit the particular site. In this regard, it would be similar to construction of a large building such as a civic centre. There is no set cost for such buildings, due to most expenses in construction being mainly dependant on the particular location, and the needs expressed by the community constructing the centre. As such, an extensive tender and bid process is the norm, and used to determine the amount of funding required for the construction of a particular civic centre, and not the buildings in general.

Likewise, the same estimation methods would be the same for these turbines, especially since scaling allows installations from capacity of a few watts to a few megawatts. Costs for each turbine would be largely determined from site characteristics, as well as duty cycle and maintenance expectations of the client.

13 Project Success

We have successfully met our design objective of designing, building and testing a unique water current energy device. The below list is a summary of the team's previously defined project objectives and the results in achieving those objectives.

As stated in our problem statement, the water current energy device had to:

1. Be designed, built and tested using available facilities: The Power Rangers Team has successfully designed three Gorlov helical turbines, fabricated components of the three turbines, assembled a water turbine and a wind turbine and completed testing of these turbines in MUN's wave/tow tank and wind tunnel.

2. Be novel in design: The team's selected concept, the Gorlov helical turbine design, is uncommon for use in the water power generation industry.

3. Successfully generate power from a flow of water**:** The fabricated water turbine achieved a maximum power output of 13 Watts during testing.

4. Be safe and environmentally friendly: Stress and fatigue analysis validated safety of turbine designs. The Gorlov helical blade design leads ample room for marine life to navigate through. However, further testing of the turbine in a long term river application is required to determine environmental effects.

5. Be self-starting: Self-starting was achieved during testing for both the water turbine and the wind turbine.

6. Be implemented locally: Due to time limitations, local implementation was removed from the project scope. Weather through the winter was much worse than expected, and we decided it was not practical, nor safe, to test the turbine in-situ. It is now future work to complete.

14 Future Work

Planned future work includes the assembly and testing of Turbine Design I. This first requires the fabrication of endplates for the turbine. Testing will be conducted in the wave/tow tank and follow the same procedure as outlined in section 10.2 Water Turbine Testing.

The design team also plans to submit an abstract to the OCEANS'14 Conference being held September 14th- 19th 2014. OCEANS'14 is a major international conference attended by scientists, engineers and responsible ocean users to discuss the latest research in Ocean Engineering and Marine Technology (26).

Moving forward the team also aims to conduct fabrication of larger turbines optimized specifically for site application. Local implementation of our turbine is the only objective not achieved. A long term test in a river setting would give the design team a good idea of the effects of environmental exposure and realistic flow patterns on the turbine.

CFD Design of experiments should be conducted to optimize turbines for maximum efficiency and power development. This would provide a formula to predict turbine performance in particular conditions, and provide an expedient method for designing turbines to client and site specifications.

Planned future work also includes developing Matlab code to allow analysis of turbine configuration without the computationally intense requirements of full CFD simulations. Essentially, this would provide a "quick and dirty" overview of expected turbine performance, allowing the proper setup of virtual models for CFD, and reducing time wasted in simulations that proved ineffective. Additionally, if results predicted by the Matlab code closely matched CFD analysis and any physical modeling, it could be developed into a useful tool for designing turbines to client specification. The basis for the future code comes from Woods' thesis entitled *Simulation of VAWT and Hydrokinetic Turbines with Variable Pitch Foils* (27) and is attached in Appendix G.

An additional step required to generate the maximum power output from the current is to implement maximum power point tracking (MPPT). A MPPT contains a switch-mode converter and a control with tracking capability. The switch-mode converter draws energy at one potential, stores this energy as magnetic energy, then releases the energy at a different potential. The switch-mode power supply can be set up as either a buck converter or boost voltage converter with the goal to provide a constant output voltage (3).

15 Summary & Conclusions

We have successfully designed, built and tested a unique water current energy device. We developed design objectives based on project goals and constraints. In completing background research we determined that while many devices have been designed to harness water current energy, lift-based turbines represent the most efficient option for power generation. To optimize performance in low-speed currents, we selected the Gorlov helical cross-flow turbine as our concept. The Gorlov helical design has been proven to perform well in water currents, and has also been the basis of design for several wind turbines.

Next, the team found an acceptable design of the Gorlov helical turbine for testing. SolidWorks 3D modeling was used to develop a virtual model for construction and virtual analysis. The starting performance and torque behavior of multiple Gorlov helical turbine designs were analyzed using computational fluid dynamics software. Blade designs varied in foil shape and solidity. FEA was also performed. From these analyses, three turbines were chosen for fabrication. The preliminary designed turbine, was fabricated by DJ Composites Inc. and gave the team insight into a comprehensive concept-to-physical design procedure for composite manufacturing. The two additional turbines, a water turbine and a wind turbine, were fabricated using rapid-prototype machines to print the ABS blades, and machined parts for blade and shaft mounting. These two turbines were subsequently tested.

The water turbine was tested in Memorial's wave/tow tank, while the wind turbine was tested in the university's wind tunnel. Trials for the water turbine were conducted for stream speeds of 0.25m/s to 2.0m/s in increments of 0.25m/s. For each speed trial, multiple tows were conducted with increasing brake torque, starting at zero (freewheel) and continuing until turbine was unable to rotate. Results of these tests were analyzed to produce Coefficient of Power vs. Coefficient of Speed, and Power vs.

Angular Velocity curves for comparison with typical turbomachinery performance curves. The wind turbine was tested to determine self-starting capabilities and TSR.

The water turbine performed slightly better than expected in power generation, with lower efficiency than targeted. The maximum power output achieved was 13 Watts. Cp vs. Cs and Power vs. ω curves closely resembled those from more traditional turbine configurations. The wind turbine demonstrated self-starting capabilities, with a lower overall TSR than typical of water turbines, indicating the potential for an air-optimized helical turbine. From the test results, we believe the turbine constructed is a good starting point for future research in optimization.

We identified issues with test apparatus that should be resolved for testing new turbines. We explored environmental, safety, maintenance, legal, and ecological risks associated with our turbine prototypes.

We kept within budget and on schedule, as shown in Appendix A, throughout the project. Our water current energy device has proven successful and we have met five out of the six project objectives. Our strong team work contributed greatly to the quality, understanding and success of our water current energy device.

References

1. **Khan, Mohammad Jahangir Alam.** *Adaptive Power Tracking Control of Hydrokinetic Energy Conversion Systems.* St.John's : Memorial University of Newfoundland, 2010. PhD Thesis.

2. **Harvey, A.** *Micro-hydro Design Manual.* s.l. : ITDG Publishing, 1992.

3. **Khan, MD Nahidul Islam.** *A Micro Seafloor Marine Current Energy Conversion System.* St.John's : Memorial Univesity of Newfoundland, 2008. Master's Thesis.

4. **Hinchey, Dr. Michael.** Power. *Fluid Power Mechanics.* [Online] 04 2013. http://www.engr.mun.ca/~mhinchey/6961/NOTES/POWER.pdf.

5. Town of Petty Harbour-Maddox Cove. *Welcome.* [Online] 02 2014. http://www.pettyharbourmaddoxcove.ca/.

6. **AMEC Earth & Environmental .** *Physical Oceanography Setting .* St. John's, Newfoundland : s.n., 2010.

7. **Oceans Ltd. .** *Physical Environmental Conditions at Fiddlehead Well Site.* St. John's, NL : s.n., 2010.

8. **Oceans Ltd.** *Wind, Waves and Currents at Mizzen.* St. John's, NL : s.n., 2008.

9. **Canadian Hydraulics Centre.** *Inventory of Canada's Marine Renewable Energy Resources.* National Research Council Canada. Ottawa : National Research Council Canada, 2006. Feasibility Study.

10. List of Stations. *Department of Environment and Conservation.* [Online] 2014. http://www.env.gov.nl.ca/wrmd/ADRS/v6/Graphs_List.asp.

11. **Team, Rescue Rangers Design.** *Mechanical Design Project I - Research and Concept Selection Report.* St. John's, NL : s.n., 2013.

12. Auger Wear Shoes/Flighting. *May Wes.* [Online] http://www.maywes.com/UHMW_auger_wear_shoes.

13. Environmental Product Agents. *Turbine Vents.* [Online] http://img3.tradeee.com/up/aipu123/100831.jpg.

14. www.hakusa.com. *wind turbine.* [Online] http://www.hakusa.com/wind/fusha/Dscf0006s.jpg.

15. Darrieus rotor. *www.Wikipedia.com.* [Online] http://upload.wikimedia.org/wikipedia/commons/d/d4/Darrieus_rotor001.jpg.

16. **Institute, Tide Mill.** Tide Mill Institute. [Online] [Cited: January 28, 2014.]

17. *Sennacherib, Archimedes, and the Water Screw: The context of Invention in the Ancient World.* **Dalley, Stephanie and Oleson, John.** 2003, Technology and Culture vol. 44, number 1.

18. The Queen goes green. *The Telegraph (UK).* [Online] 9 2011. http://www.telegraph.co.uk/news/uknews/theroyalfamily/8749107/The-Queen-goes-green-hydroelectric-turbines-arrive-at-Windsor-Castle.html.

19. *Archimedes Screws For Microhydro Power Generation.* **Murray Lyons, William David Lubitz.** Minneapolis, MN : s.n., 2013. Energy Sustainability & 11th Fuel Cell Science, Engineering and Technology Conference. p. 7.

20. *Twisted Turbine.* **Jahangir Alam, Tariq Iqbal.** 2010, The Journal of Ocean Technology.

21. **Gorlov, A.M.** *Unidirectional helical reaction turbine operable under reversible fluid flow for power systems. 5451137* U.S., 1995.

22. **Chandima Perera, Ryan Oliver, Nicholas Wasmeier, Christopher Rossiter.** *Selection of Turbine Type For In-Stream Micro Hydro Applications in Remote Areas.* St. John's, NL : s.n., 2010.

23. *Limits of the Turbine Efficiency for Free Fluid Flow.* **Alexander N. Gorban, Alexander M. Gorlov, Valentin M. Silantyev.** s.l. : Journal of Energy Resources Technology, 2001, Journal of Energy Resources Technology, p. 1.

24. **Wikipedia.** Boundary Layer- Wikipedia, the free encyclopedia. [Online] Wikipedia, February 21, 2014. [Cited: March 04, 2014.] http://en.wikipedia.org/wiki/Boundary_layer.

25. Oceans 14. [Online] April 2014, 1. http://www.oceans14mtsieeestjohns.org/.

26. **Woods, L.D.** "Simulation of VAWT and Hydrokinetic Turbines with Variable Pitch Foils,". Boise : M.S. thesis, B.S.U, 2013.

27. **Wikipedia.** Vortex Generator - Wikipedia, the free encyclopedia. [Online] Wikipedia, February 28, 2014. [Cited: March 04, 2014.] http://en.wikipedia.org/wiki/Vortex_generator.

28. **Victoria, University of.** Wave Energy Converter Test. [Online] March 1, 2014. http://www.uvic.ca/research/projects/wcwi/home/news/current/news-story-4.php.

29. *Grab Cad.* [Online] [Cited: February 1, 2014.] http://www.grabcad.com.

Appendix A Project Management Plan

The project management plan consists of the division of team member responsibilities and the project timeline.

Team Member Responsibilities

Strengths were subdivided based on the strengths of each team member. Below the team's organizational chart is shown.

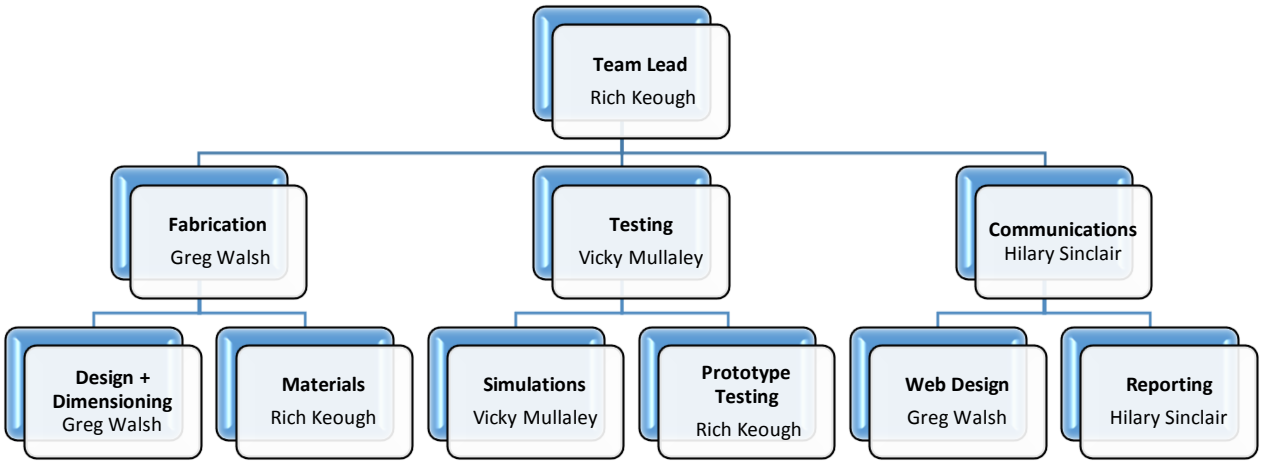

Figure 38:Organizational Chart

Team lead is responsible to ensure the design process runs smoothly, by keeping all members focused and on task. This involves monitoring the design schedule, budget and leading all team meetings.

Fabrication Team is responsible for the design and dimensioning of the water current energy device. This also includes material selection and corrosion resistance.

Testing Team is responsible for testing the designed water current energy device using software simulations. After the prototype is fabricated they will next facilitate prototype testing on the flume tank and record the results using a data acquisition system.

Communication Team is responsible for building a detailed working website to display the progress of our project. In addition they are responsible for formatting of final report submissions and presentations.

Project Schedule

The Plan

ID	Task Name	Duration	Start	Finish
1	**Milestones**	**68 days**	**Wed 1/15/14**	**Tue 4/8/14**
2	Kickoff Meeting	0 days	Wed 1/15/14	Wed 1/15/14
3	Project Plan and Baselines Complete	0 days	Tue 1/21/14	Tue 1/21/14
4	Concept Selection Complete	0 days	Sat 1/25/14	Sat 1/25/14
5	Prototype Preliminary Design Complete	22 days	Sat 2/8/14	Fri 4/4/14
6	CFD Complete	0 days	Sun 3/2/14	Sun 3/2/14
7	FEA Complete	0 days	Sun 3/2/14	Sun 3/2/14
8	Prototype Fabrication Complete	0 days	Fri 3/28/14	Fri 3/28/14
9	Testing Complete	0 days	Sat 3/15/14	Sat 3/15/14
10	Final Report	0 days	Tue 4/8/14	Tue 4/8/14
11	**Team Organization and Development**	**5 days?**	**Wed 1/15/14**	**Mon 1/20/14**
12	Determine Team Organization Structure	3 days	Wed 1/15/14	Fri 1/17/14
13	Assign Team Roles	5 days?	Wed 1/15/14	Mon 1/20/14
14	**Communication & Documentation**	**68 days?**	**Fri 1/17/14**	**Fri 4/11/14**
15	**Website**	**68 days**	**Fri 1/17/14**	**Fri 4/11/14**
16	Design and Layout Selection	0 days	Tue 1/21/14	Tue 1/21/14
17	Website Functional	0 days	Tue 1/28/14	Tue 1/28/14
18	**Upload Meeting Minutes**	**68 days**	**Fri 1/17/14**	**Fri 4/11/14**
32	**Reports & Presentations**	**55 days?**	**Thu 1/30/14**	**Tue 4/8/14**
33	**Presentation & Report 1**	**7 days?**	**Thu 1/30/14**	**Fri 2/7/14**

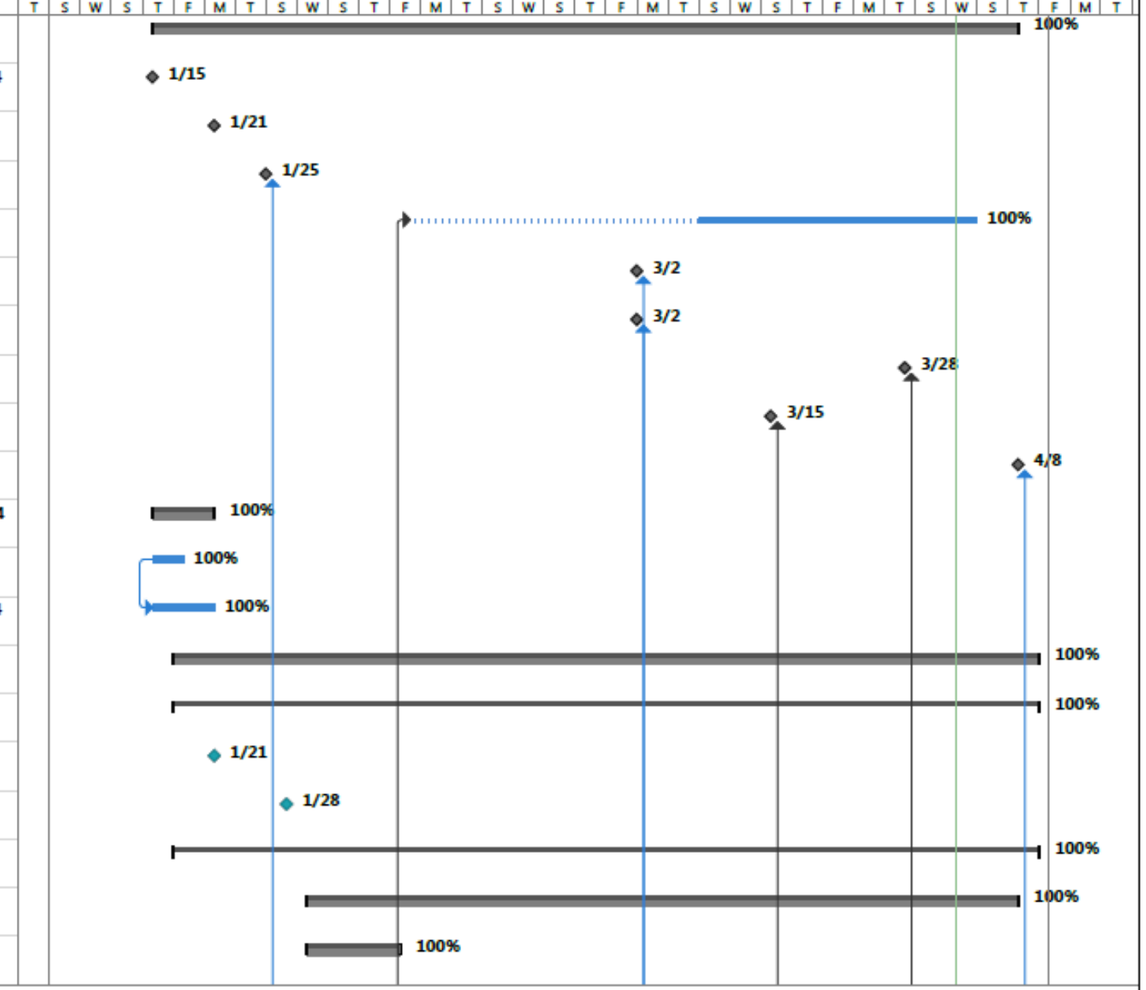

Critical | Critical Split | Critical Progress | Task | Split | Task Progress | Manual Task | Start-only | Finish-only | Duration-only | Baseline | Baseline Split | Baseline Milestone | Milestone | Summary Progress | Summary | Manual Summary | Project Summary | External Tasks | External Milestone | Inactive Task | Inactive Milestone | Inactive Summary | Deadline

Page 1

Figure 39: Project Schedule (1/3)

The Plan

ID		Task Mode	Task Name	Duration	Start	Finish
34	✓		Prepare Information	1 day	Thu 1/30/14	Thu 1/30/14
35	✓		Write Report	5 days	Fri 1/31/14	Thu 2/6/14
36	✓		Edits	1 day?	Fri 2/7/14	Fri 2/7/14
37	✓		Final Draft Complete / Submitted	0 days	Fri 2/7/14	Fri 2/7/14
38	✓		**Presentation & Report 2**	**7 days?**	**Thu 2/27/14**	**Wed 3/5/14**
39	✓		Prepare Information	1 day	Thu 2/27/14	Thu 2/27/14
40	✓		Write Report	5 days	Fri 2/28/14	Tue 3/4/14
41	✓		Edits	1 day?	Wed 3/5/14	Wed 3/5/14
42	✓		Final Draft Complete / Submitted	0 days	Wed 3/5/14	Wed 3/5/14
43	✓		**Final Presentation & Report**	**7 days?**	**Mon 3/31/14**	**Tue 4/8/14**
44	✓		Prepare Information	1 day	Mon 3/31/14	Mon 3/31/14
45	✓		Write Report	5 days	Tue 4/1/14	Mon 4/7/14
46	✓		Edits	1 day?	Tue 4/8/14	Tue 4/8/14
47	✓		Final Draft Complete / Submitted	0 days	Tue 4/8/14	Tue 4/8/14
48	✓		**Concept Development**	**17 days?**	**Sun 1/5/14**	**Sat 1/25/14**
49	✓		Brainstorming	9 days	Sun 1/5/14	Wed 1/15/14
50	✓		Background Research	8 days	Wed 1/15/14	Thu 1/23/14
51	✓		Concept Development	8 days	Wed 1/15/14	Thu 1/23/14
52	✓		Concept Evaluation	1 day?	Fri 1/24/14	Fri 1/24/14
53	✓		Concept Selection	1 day?	Sat 1/25/14	Sat 1/25/14

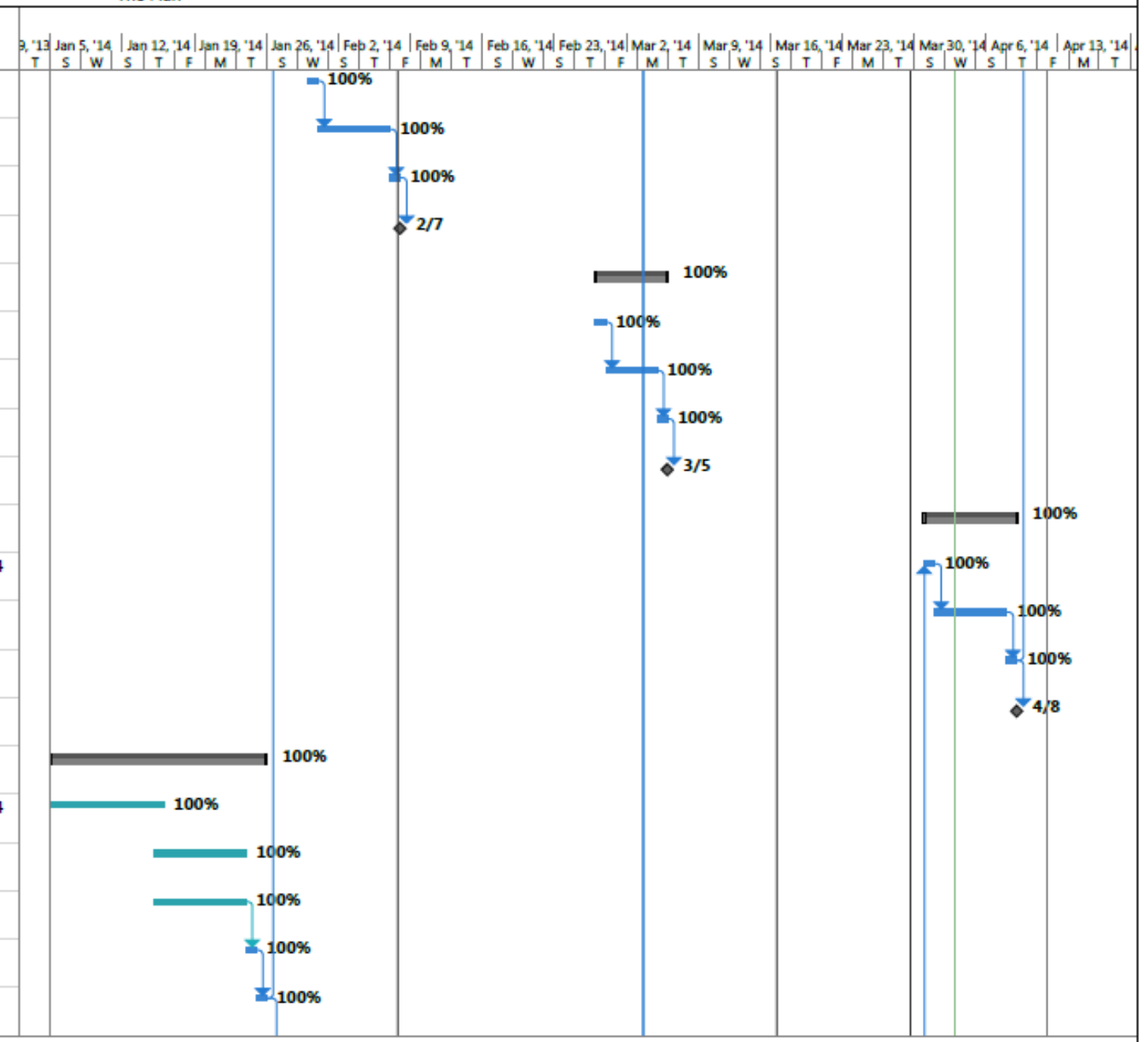

Critical | Critical Split | Critical Progress | Task | Split | Task Progress | Manual Task | Start-only | Finish-only | Duration-only | Baseline | Baseline Split | Baseline Milestone | Milestone | Summary Progress | Summary | Manual Summary | Project Summary | External Tasks | External Milestone | Inactive Task | Inactive Milestone | Inactive Summary | Deadline

Page 2

Figure 40: Project Schedule (2/3)

The Plan

ID		Task Mode	Task Name	Duration	Start	Finish
54	✓		**Prototype Design**	**34 days?**	**Mon 1/27/14**	**Fri 3/7/14**
55	✓		Turbine design	25 days?	Mon 1/27/14	Fri 2/28/14
56	✓		Test chassis design	8 days?	Fri 2/28/14	Fri 3/7/14
57	✓		**Computer Analysis**	**10 days?**	**Thu 2/20/14**	**Sun 3/2/14**
58	✓		CFD Analysis	10 days?	Thu 2/20/14	Sun 3/2/14
59	✓		FEA Analysis	8 days?	Sun 2/23/14	Sun 3/2/14
60	✓		**Prototype Fabrication**	**15 days?**	**Tue 3/11/14**	**Fri 3/28/14**
61	✓		Turbine Mount Fabrication	15 days?	Tue 3/11/14	Fri 3/28/14
62	✓		Turbine Blade Fabrication	15 days?	Tue 3/11/14	Fri 3/28/14
63	✓		**Physical Prototype Testing**	**7 days?**	**Sun 3/9/14**	**Sat 3/15/14**
64	✓		Tow Tank Testing	7 days?	Sun 3/9/14	Sat 3/15/14
65	✓		Design Performance Analysis & Refinements for Final Report	10 days?	Mon 3/17/14	Fri 3/28/14

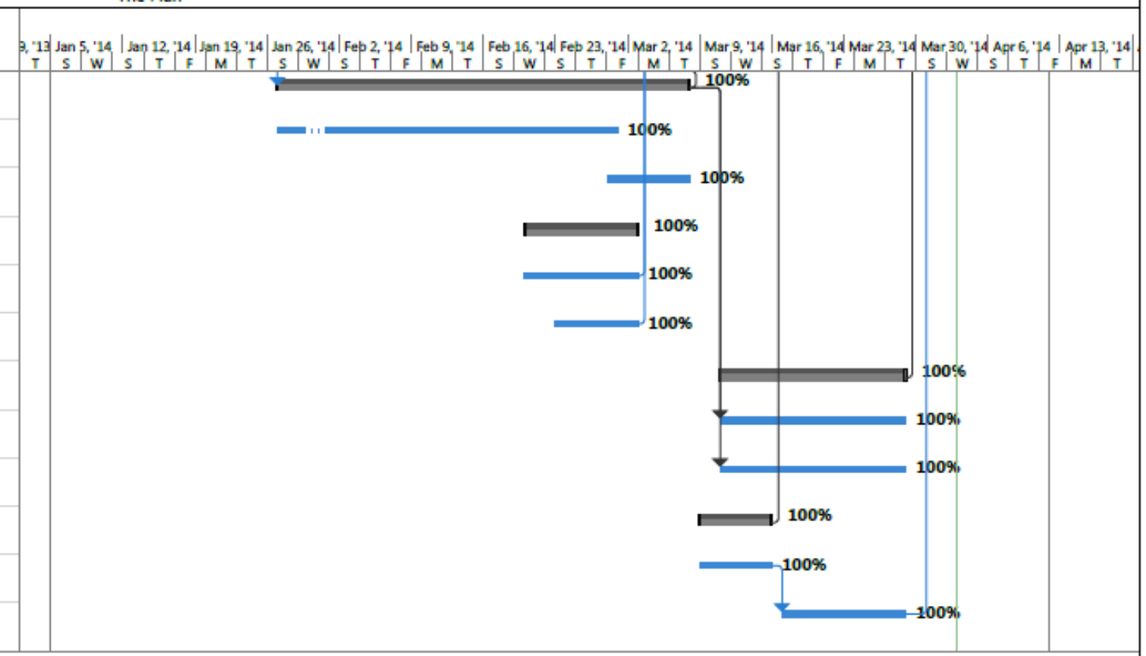

Critical		Split		Finish-only		Baseline Milestone		Manual Summary		Inactive Task	
Critical Split		Task Progress		Duration-only		Milestone		Project Summary		Inactive Milestone	
Critical Progress		Manual Task		Baseline		Summary Progress		External Tasks		Inactive Summary	
Task		Start-only		Baseline Split		Summary		External Milestone		Deadline	

Page 3

Figure 41: Project Schedule (3/3)

Appendix B Tidal Current Sites in Newfoundland

Site Name	Latitude	Longitude	Maximum Current Speed Flood	Maximum Current Speed Ebb	Mean Maximum Depth Average Current Speed	Mean Power Density	Width of Passage	Average Depth of Passage	Flow Cross-sectional Area	Mean Potential Power
	deg	deg	knot	m/s	m/s	kW/m^2	m	m	m^2	MW
Strait of Belle Isle	51.45	-56.68			-	0.20	26,069	49	1,298,236	373
Forteau	51.41	-56.95	4	5	1.97	0.89	1,500	35	53,700	48
Pointe Armour	51.45	-56.86	4	5	1.97	0.89	1,500	35	53,700	48
Cape Bauld	51.64	-55.43	2	2	0.88	0.08	2,000	15	31,600	2
Cape Anguille	47.90	-59.41	3	3	1.31	0.26	700	10	7,700	2
Stearing Island	49.93	-57.81	2	2	0.88	0.08	1,650	13	23,100	2
Cape St George	48.46	-59.28	3	3	1.31	0.26	200	18	3,800	1
Pass Island Tickle	47.50	-56.19	4	3	1.53	0.42	300	7	2,490	1
Placentia Gut	47.25	-53.96	9	9	3.94	7.12	80	3	336	2
Pike Run	54.10	-58.36	6	5	2.41	1.63	580	45	26,680	43
Cul-de-Sac	54.06	-58.56	6	5	2.41	1.63	360	14	5,400	9
Cap Islet	56.55	-61.45	4	5	1.97	0.89	610	9	6,100	5
Goose Bay Narrows	54.43	-59.99	3	5	1.75	0.63	813	7	6,504	4
The Narrows	53.67	-57.07	3.5	3.5	1.53	0.42	260	18	4,940	2
Bridges Passage	56.45	-61.56	4	4	1.75	0.63	280	5	1,680	1
									Total:	544

Table 8: Tidal Current Sites in Newfoundland and Labrador (9)

Appendix C Generator Power Test

Testing of a proposed generator was carried out simply to test its capability to generate power with reasonable rotational speeds. For the test, the motor/generator was driven by an 18v cordless drill at 1,500 RPM while voltage drop across a variable resistor was measured. The test set-up is shown below, in Figure 42.

Figure 42: Power Test Set-up

From this test, we recorded the results shown in Figure 43. These results indicate that the generator is not optimal, as power generated tends to decrease with added load, possibly due to the low internal resistance of the motor. However, the amount of power created is not a critical measurement so this equipment will still serve the purpose of creating some current from the turbine rotation in order to demonstrate effective electrical generation. The actual power output of the fabricated turbines will instead be measured via brake torque. The results of the motor test are shown in Table 9.

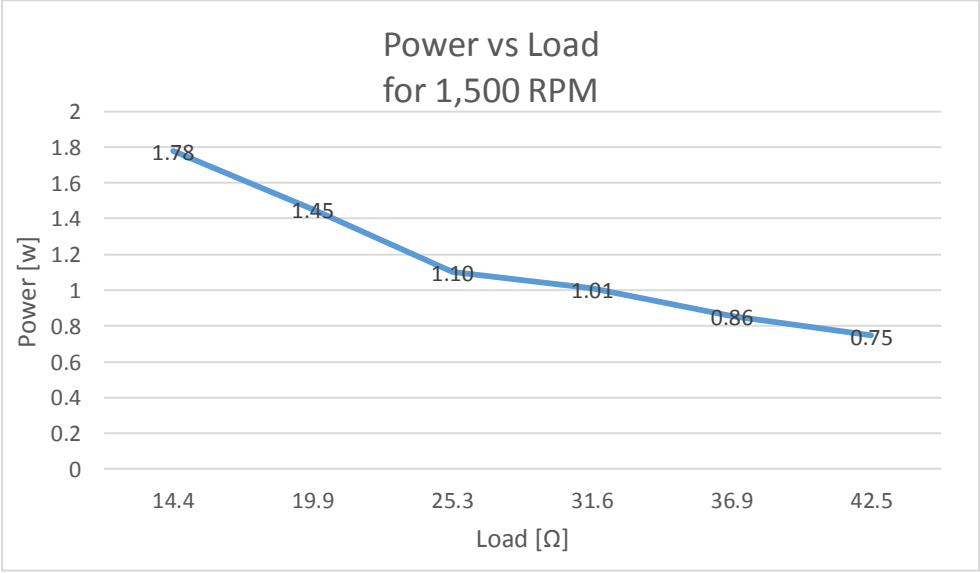

Figure 43: Power vs. Load Results from Motor Test

Figure 44: Turbine Motor/Generator

Table 9: Power generated from motor test

For motor with internal resistance of 9.8 ohms, at RPM = 1,500			
14.4	5.75	0.399306	2.296007
19.9	5.95	0.298995	1.77902
25.3	6.06	0.239526	1.451526
31.6	5.9	0.186709	1.101582
36.9	6.1	0.165312	1.008401
42.5	6.03	0.141882	0.855551
50.4	6.13	0.121627	0.745573

Appendix D Composite Blade Fabrication Drawing

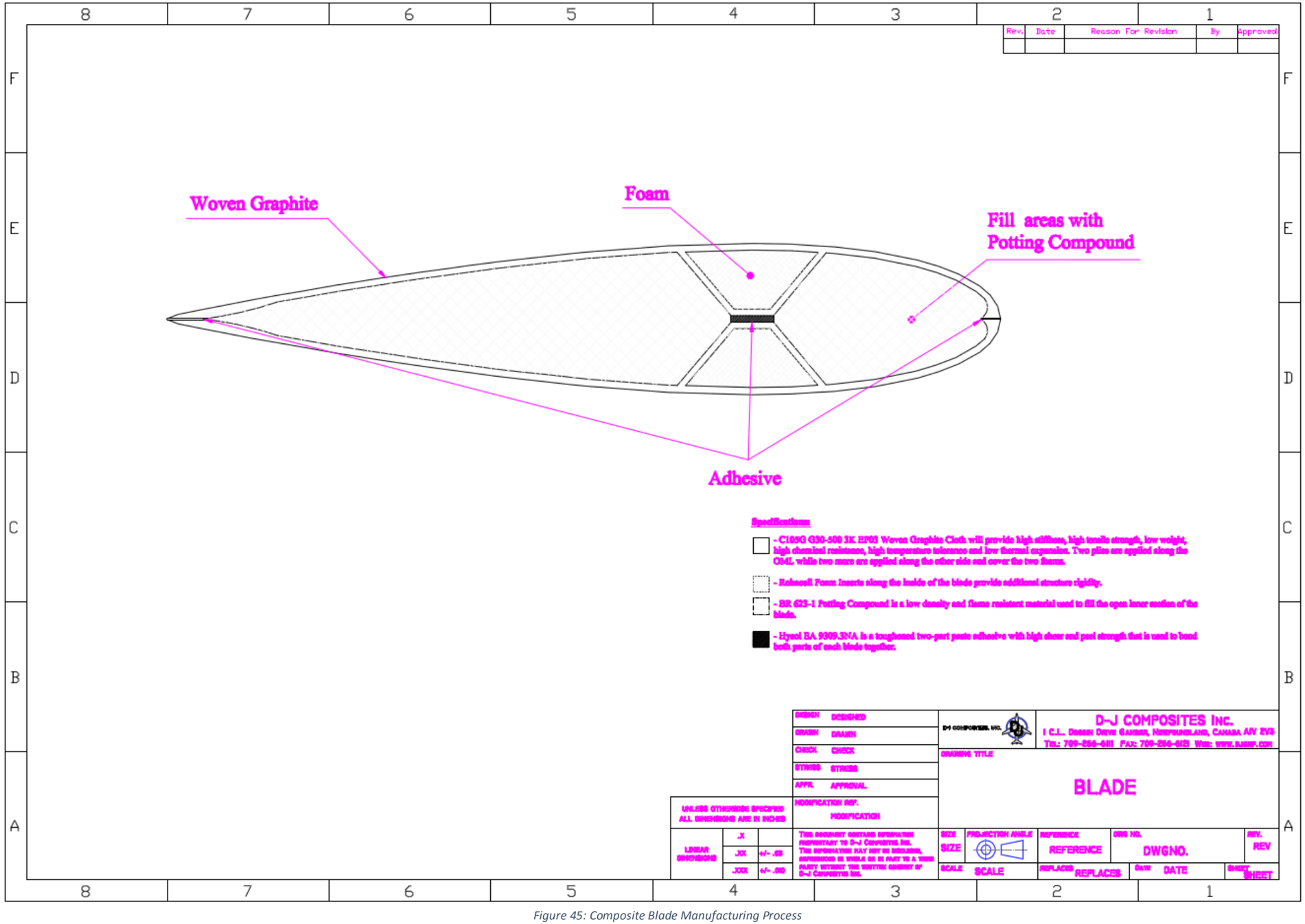

Figure 45: Composite Blade Manufacturing Process

Appendix E Water Turbine Testing Results

Table 10: Water Turbine Testing Results

Run	Flow Speed(m/s)	Torque(Nm)	Angular Velocity(RPS)	Angular Velocity(rad/s)	Power(W)	Cp	Cs
A1	0.250	0.005	0.124	0.779	0.004	0.012	0.623
B1	0.750	0.000	0.873	5.487	0.000	0.000	1.463
B2	0.750	0.074	0.666	4.184	0.308	0.037	1.116
B3	0.750	0.109	0.633	3.974	0.432	0.051	1.060
B4	0.750	0.155	0.597	3.750	0.582	0.069	1.000
B5	0.750	0.196	0.487	3.062	0.600	0.071	0.816
B6	0.750	0.237	0.000	0.000	0.000	0.000	0.000
C1	1.000	0.000	1.208	7.589	0.000	0.000	1.518
C2	1.000	0.074	1.091	6.853	0.505	0.025	1.371
C3	1.000	0.237	0.992	6.232	1.476	0.074	1.246
C4	1.000	0.418	0.820	5.151	2.151	0.108	1.030
C5	1.000	0.604	0.503	3.162	1.910	0.096	0.632
C6	1.000	0.680	0.000	0.000	0.000	0.000	0.000
D1	1.250	0.000	1.525	9.584	0.000	0.000	1.533
D2	1.250	0.301	1.405	8.830	2.658	0.068	1.413
D3	1.250	0.528	1.259	7.911	4.180	0.107	1.266
D4	1.250	0.738	0.990	6.222	4.593	0.118	0.995
D5	1.250	0.826	0.754	4.739	3.913	0.100	0.758
D6	1.250	0.942	0.000	0.000	0.000	0.000	0.000
E1	1.500	0.000	1.863	11.704	0.000	0.000	1.561
E2	1.500	0.348	1.741	10.941	3.804	0.056	1.459
E3	1.500	0.598	1.644	10.330	6.180	0.092	1.377
E4	1.500	0.826	1.414	8.887	7.338	0.109	1.185
E5	1.500	0.948	1.255	7.885	7.476	0.111	1.051
E6	1.500	1.030	1.198	7.525	7.749	0.115	1.003
E7	1.500	1.117	0.000	0.000	0.000	0.000	0.000
F1	1.750	0.000	2.160	13.572	0.000	0.000	1.551
F2	1.750	0.359	2.023	12.711	4.567	0.043	1.453
F3	1.750	0.651	1.914	12.026	7.826	0.073	1.374
F4	1.750	0.966	1.653	10.389	10.031	0.094	1.187
F5	1.750	1.263	1.305	8.200	10.356	0.097	0.937
F6	1.750	1.397	0.753	4.729	6.606	0.062	0.540
F7	1.750	1.525	0.000	0.000	0.000	0.000	0.000
G1	2.000	0.000	2.439	15.322	0.000	0.000	1.532
G2	2.000	0.359	2.343	14.722	5.289	0.033	1.472
G3	2.000	0.651	2.202	13.837	9.005	0.056	1.384
G4	2.000	0.797	2.117	13.301	10.595	0.066	1.330
G5	2.000	0.966	2.056	12.920	12.476	0.078	1.292
G6	2.000	1.088	1.719	10.801	11.752	0.073	1.080
G7	2.000	1.234	1.638	10.293	12.700	0.079	1.029
G8	2.000	1.380	1.454	9.136	12.603	0.079	0.914
G9	2.000	1.525	1.185	7.442	11.352	0.071	0.744
G10	2.000	1.671	0.955	6.002	10.030	0.063	0.600
G11	2.000	1.817	0.000	0.000	0.000	0.000	0.000

Appendix F Magnetic Brake Specification Sheet

magnetic particle BRAKE B35 — 0.6 to 35 lb.-in.

DATA SHEET

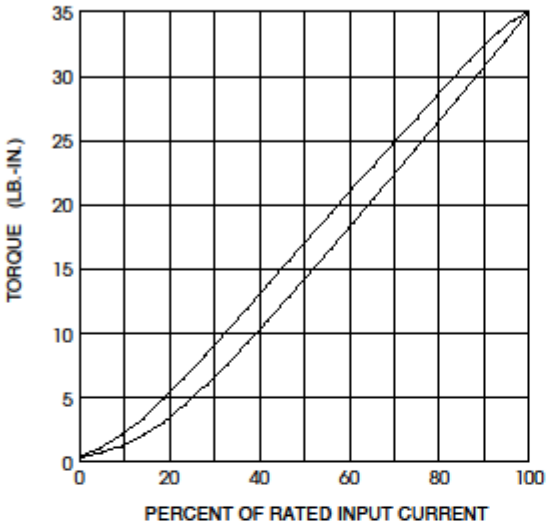

CHARACTERISTICS - With no electrical excitation, the shaft freely rotates. With electrical excitation, the shaft becomes coupled to the housing. Torque is proportional to input current (see torque graph), and independent of RPM. While the load torque is less than the output torque, the shaft won't rotate. When the load torque is increased, the brake will slip smoothly at the torque level set by the coil input current.

Torque range	0.6 to 35	lb.-in.
Maximum RPM	1800	RPM
Maximum heat dissipation	30	watts
Maximum case temperature	160	degrees F
Maximum overhung load	50	lbs.
Shaft inertia	12×10^{-5}	lb.-in.-sec^2
Response (unforced)	35	mSec.
Response (forced)	20	mSec.
Weight	4	lbs.

← Use the lower curve when approaching a current value from 0 amps. Use the upper curve when approaching a current value from 100% rated current.

	6 V	12 V	24 V	90 V
COIL RESISTANCE (ohms)	4.4	17	65	830
100% INPUT CURRENT (amps)	1.3	0.67	0.35	0.10

← Rated D.C. coil voltages available: 6 VDC (yellow leads), 12 VDC (green leads), 24 VDC (red leads), 90 VDC (blue leads).

BRAKE PERFORMANCE

TORQUE: At the rated voltage, the brake will draw 100% of the rated input current. Output torque will be 35 lb.-in.

POWER SUPPLY: A "constant-current" D.C. power supply is recommended for the best accuracy in open-loop control systems. This type of power supply will maintain a fixed (but adjustable) output current, regardless of the temperature of the brake, so output torque is constant (but adjustable).

HEAT DISSIPATION: The brake can dissipate 30 slip (thermal) watts continuously. For continuous slip, calculate the heat input by the formula :

HEAT (watts) = RPM x TORQUE (lb.-in.) x 0 .012

Using the above formula: At rated torque, the maximum continuous slip RPM is 71. The brake can dissipate higher amounts of heat for short periods of time, but the average must not exceed 30 watts. The case temperature must never exceed 160 degrees F.

INSTALLATION INFORMATION

Do not drop, or strike with a hammer. Keep away from fine metal filings and fine metal chips. Shield from liquids.

Do not attempt to remove the brake shaft or retaining rings.

All pulleys, sprockets, couplings, thru-shafts (hollow shaft models), etc. must mount as slide fits. Use a puller to remove stuck components. Never pry or hammer to install or remove components.

Solid Shaft Models: Center your set-screw on the flat of the brake shaft.

Hollow Shaft Models: Never tighten the #10 set screws of the clamp ring without the thru-shaft installed. Tighten set screws to 36 in.-lbs.

Always use a flexible coupling when connecting the shaft of a rigidly mounted brake to the shaft of another rigidly mounted device. Precisely align both shafts.

Always electrically ground the brake.

Placid Industries, Inc. www.placidindustries.com
139 Mill Pond Drive, Lake Placid, NY 12946 USA Phone 518 523-2422 Fax 518 523-2746
1/95

Appendix G MATLAB CODE